ELSEVIER

Journal of Neuroscience Methods 141 (2005) 171–198

JOURNAL OF NEUROSCIENCE METHODS

www.elsevier.com/locate/jneumeth

Invited review

Electrical stimulation of excitable tissue: design of efficacious and safe protocols

Daniel R. Merrill[a,*], Marom Bikson[b], John G.R. Jefferys[c]

[a] *Department of Bioengineering, University of Utah, 20 South 2030 East, Biomedical Polymers Research Building, Room 108G, Salt Lake City, UT 84112-9458, USA*

[b] *Department of Biomedical Engineering, City College of New York, New York, NY, USA*

[c] *Division of Neuroscience (Neurophysiology), School of Medicine, The University of Birmingham, Birmingham B15 2TT, UK*

Accepted 12 October 2004

Abstract

The physical basis for electrical stimulation of excitable tissue, as used by electrophysiological researchers and clinicians in functional electrical stimulation, is presented with emphasis on the fundamental mechanisms of charge injection at the electrode/tissue interface. Faradaic and non-Faradaic charge transfer mechanisms are presented and contrasted. An electrical model of the electrode/tissue interface is given. The physical basis for the origin of electrode potentials is given. Various methods of controlling charge delivery during pulsing are presented. Electrochemical reversibility is discussed. Commonly used electrode materials and stimulation protocols are reviewed in terms of stimulation efficacy and safety. Principles of stimulation of excitable tissue are reviewed with emphasis on efficacy and safety. Mechanisms of damage to tissue and the electrode are reviewed.

Keywords: Efficacy; Electrode; Interface; Protocol; Safety; Stimulation

Contents

* Corresponding author. Tel.: +1 801 585 0791; fax: +1 801 581 5151.
E-mail address: dan.merrill@utah.edu (D.R. Merrill).

0165-0270/$ – see front matter © 2004 Elsevier B.V. All rights reserved.
doi:10.1016/j.jneumeth.2004.10.020

1. Physical basis of the electrode/electrolyte interface

Electrical stimulation and recording of excitable tissue is the basis of electrophysiological research and clinical functional electrical stimulation, including deep brain stimulation and stimulation of muscles, peripheral nerves or sensory systems. When a metal electrode is placed inside a physiological medium such as extracellular fluid (ECF), an interface is formed between the two phases. In the metal electrode phase and in attached electrical circuits, charge is carried by electrons. In the physiological medium, or in more general electrochemical terms the electrolyte, charge is carried by ions, including sodium, potassium, and chloride in the ECF. The central process that occurs at the electrode/electrolyte interface is a transduction of charge carriers from electrons in the metal electrode to ions in the electrolyte. The purpose of this review is to introduce the electrochemical processes occurring at this interface during electrical stimulation of excitable tissue and to analyze the properties of stimulation waveforms and electrode materials used in neuroscience research and clinical applications. Throughout the review, we will illustrate how the choice of electrode material and stimulation methodology can profoundly influence the results of acute and chronic electrophysiological studies, as well as safety during clinical stimulation.

In the simplest system, two electrodes are placed in an electrolyte, and electrical current passes between the electrodes through the electrolyte. One of the two electrodes is termed a working electrode (WE), and the second is termed a counter electrode (CE). The working electrode is defined as the electrode that one is interested in studying, with the counter electrode being necessary to complete the circuit for charge conduction. An electrophysiology experiment may also contain a third electrode termed the reference electrode (RE), which is used to define a reference for electrical potential measurements.

A change in electrical potential occurs upon crossing from one conducting phase to another (from the metal electrode to the electrolyte) at the interface itself, in a very narrow interphase region, thus forming an electric field (measured in V/m) at the interface. This change in potential exists even in the equilibrium condition (no current). Electrochemical reactions may occur in this interphase region if the electrical potential profile is forced away from the equilibrium condition. In the absence of current, the electrical potential is constant (no gradient) throughout the electrolyte beyond the narrow interphase region. During current flow, a potential gradient exists in the electrolyte, generally many orders of magnitude smaller than at the interface.

There are two primary mechanisms of charge transfer at the electrode/electrolyte interface, illustrated in Fig. 1. One is a non-Faradaic reaction, where no electrons are transferred between the electrode and electrolyte. Non-Faradaic reactions include redistribution of charged chemical species in the electrolyte. The second mechanism is a Faradaic reaction, in which electrons are transferred between the electrode and electrolyte, resulting in reduction or oxidation of chemical species in the electrolyte.

1.1. Capacitive/non-Faradaic charge transfer

If only non-Faradaic redistribution of charge occurs, the electrode/electrolyte interface may be modeled as a simple electrical capacitor called the double layer capacitor C_{dl}. This capacitor is formed due to several physical phenomena (von Helmholtz, 1853; Guoy, 1910; Chapman, 1913; Stern, 1924; Grahame, 1947). First, when a metal electrode is placed in an electrolyte, charge redistribution occurs as metal ions in the electrolyte combine with the electrode. This involves a transient (not steady-state) transfer of electrons between the two phases, resulting in a plane of charge at the surface of the metal electrode, opposed by a plane of opposite charge, as "counterions", in the electrolyte. A second reason for formation of the double layer is that some chemical species such as halide anions may specifically adsorb to the solid electrode, acting to separate charge. A third reason is that polar molecules such as water may have a preferential orientation at the interface, and the net orientation of polar molecules separates charge.

If the net charge on the metal electrode is forced to vary (as occurs during stimulation), a redistribution of charge occurs in the solution. Suppose that two metal electrodes are immersed in an electrolytic salt solution. Next, a voltage source is applied across the two electrodes so that one electrode is driven to a relatively negative potential and the other

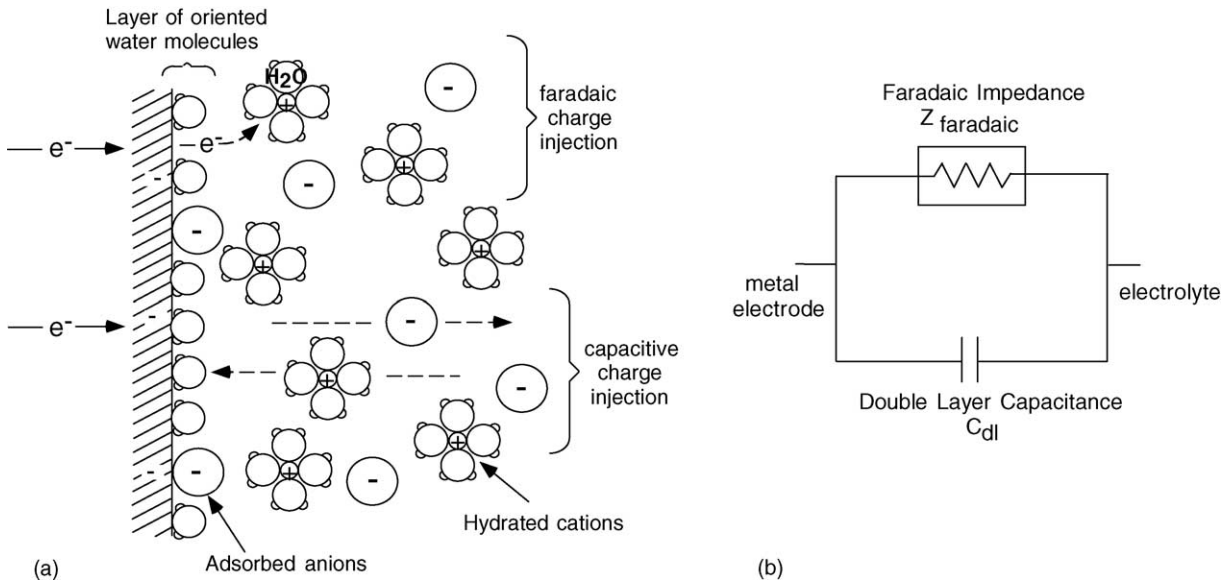

Fig. 1. The electrode/electrolyte interface, illustrating Faradaic charge transfer (top) and capacitive redistribution of charge (bottom) as the electrode is driven negative: (a) physical representation; (b) two-element electrical circuit model for mechanisms of charge transfer at the interface. The capacitive process involves reversible redistribution of charge. The Faradaic process involves transfer of electrons from the metal electrode, reducing hydrated cations in solution (symbolically $O + e^- \rightarrow R$, where the cation O is the oxidized form of the redox couple O/R). An example reaction is the reduction of silver ions in solution to form a silver plating on the electrode (reaction (1.8a)). Faradaic charge injection may or may not be reversible.

to a relatively positive potential. At the interface that is driven negative, the metal electrode has an excess of negative charge (Fig. 1). This will attract positive charge (cations) in solution towards the electrode and repel negative charge (anions). In the interfacial region, there will be net electroneutrality, because the negative charge excess on the electrode surface will equal the positive charge in solution near the interface. The bulk solution will also have net electroneutrality. At the second electrode, the opposite processes occur, i.e. the repulsion of anions by the negative electrode is countered by attraction of anions at the positive electrode. If the total amount of charge delivered is sufficiently small, only charge redistribution occurs, there is no transfer of electrons across the interface, and the interface is well modeled as a simple capacitor. If the polarity of the applied voltage source is then reversed, the direction of current is reversed, the charge redistribution is reversed, and charge that was injected from the electrode into the electrolyte and stored by the capacitor may be recovered.

1.2. Faradaic charge transfer and the electrical model of the electrode/electrolyte interface

Charge may also be injected from the electrode to the electrolyte by Faradaic processes of reduction and oxidation, whereby electrons are transferred between the two phases. Reduction, which requires the addition of an electron, occurs at the electrode that is driven negative, while oxidation, requiring the removal of an electron, occurs at the electrode that is driven positive. Unlike the capacitive mechanism, Faradaic charge injection forms products in solution that cannot be recovered upon reversing the direction of current if the products diffuse away from the electrode. Fig. 1(b) illustrates a simple electrical circuit model of the electrode/electrolyte interface, consisting of two elements (Randles, 1947; Gileadi et al., 1975; Bard and Faulkner, 1980). C_{dl} is the double layer capacitance, representing the ability of the electrode to cause charge flow in the electrolyte without electron transfer. $Z_{Faradaic}$ is the Faradaic impedance, representing the Faradaic processes of reduction and oxidation where electron transfer occurs between the electrode and electrolyte. One may generally think of the capacitance as representing charge storage, and the Faradaic impedance as representing charge dissipation.

The following are illustrative examples of Faradaic electrode reactions that may occur. Cathodic processes, defined as those where reduction of species in the electrolyte occur as electrons are transferred from the electrode to the electrolyte, include such reactions as:

$$2H_2O + 2e^- \rightarrow H_2\uparrow + 2OH^- \quad \text{(reduction of water)} \quad (1.1)$$

$$Fe^{3+} + e^- \leftrightarrow Fe^{2+} \quad \text{(simple electron transfer)} \quad (1.2)$$

$$Cu^{2+} + 2e^- \leftrightarrow Cu \quad \text{(Cu metal deposition)} \quad (1.3)$$

$$PtO + 2H^+ + 2e^- \leftrightarrow Pt + H_2O \quad \text{(oxide formation and reduction)} \quad (1.4)$$

$$IrO + 2H^+ + 2e^- \leftrightarrow Ir + H_2O \quad \text{(oxide formation and reduction)} \quad (1.5a)$$

$$IrO_2 + 4H^+ + 4e^- \leftrightarrow Ir + 2H_2O$$
(oxide formation and reduction) (1.5b)

$$2IrO_2 + 2H^+ + 2e^- \leftrightarrow Ir_2O_3 + H_2O$$
(oxide formation and reduction) (1.5c)

$$Pt + H^+ + e^- \leftrightarrow Pt\text{–}H$$ (hydrogen atom plating) (1.6)

$$M^{(n+1)+}(OH)_{(n+1)} + H^+ + e^- \leftrightarrow M^{n+}(OH)_n + H_2O$$
(valency changes within an oxide) (1.7)

$$Ag^+ + e^- \leftrightarrow Ag$$ (reduction of silver ions) (1.8a)

$$AgCl \leftrightarrow Ag^+ + Cl^-$$
(dissolution of silver chloride) (1.8b)

Anodic processes, defined as those where oxidation of species in the electrolyte occur as electrons are transferred to the electrode, include:

$$2H_2O \rightarrow O_2\uparrow + 4H^+ + 4e^-$$ (oxidation of water) (1.9)

$$Pt + 4Cl^- \rightarrow [PtCl_4]^{2-} + 2e^-$$ (corrosion) (1.10)

$$2Cl^- \rightarrow Cl_2\uparrow + 2e^-$$ (gas evolution) (1.11)

$$Fe \rightarrow Fe^{2+} + 2e^-$$ (anodic dissolution) (1.12)

$$2Ag + 2OH^- \leftrightarrow Ag_2O + H_2O + 2e^-$$
(oxide formation) (1.13)

Reaction (1.1) is the irreversible reduction of water (which is typically abundant as a solvent at 55.5 M), forming hydrogen gas and hydroxyl ions. The formation of hydroxyl raises the pH of the solution. Reversible reactions, where species remain bound or close to the electrode surface, are demonstrated by reactions (1.2)–(1.8). In reaction (1.2), the electrolyte consists of ferric and ferrous ions. By driving the metal electrode to more negative potentials, electrons are transferred to the ferric ions, forming ferrous ions. In reaction (1.3), a copper metal electrode is immersed in a solution of cuprous ions. The cuprous ions in the solution are reduced, building up the copper electrode. Reactions (1.4) and (1.5a)–(1.5c) are the reversible formation and subsequent reduction of an oxide layer on platinum and iridium, respectively. Reaction (1.6) is reversible adsorption of hydrogen onto a platinum surface, responsible for the so-called pseudocapacity of platinum. Reaction (1.7) is the general form of reversible valency changes that occur in a multilayer oxide film of iridium, ruthenium or rhodium, with associated proton or hydroxyl ion transfer (Rand and Woods, 1974; Frazer and Woods, 1979; Gottesfeld, 1980; Dautremont-Smith, 1982). Reactions (1.8a) and (1.8b) are the reversible reactions of a silver chloride electrode driven cathodically. Silver ions in solution are reduced to solid silver on the electrode (reaction (1.8a)). To maintain the solubility constant $K_S \equiv (a_{Ag^+})(a_{Cl^-})$, where a is the ionic activity, as silver ions in solution are reduced the AgCl salt covering the electrode dissolves to form silver and chloride ions in solution (reaction (1.8b)) (these reactions are discussed in more detail at the end of this section). In reaction (1.9), water molecules are irreversibly oxidized, forming oxygen gas and hydrogen ions, and thus lowering the pH. Reaction (1.10) is the corrosion of a platinum electrode in a chloride-containing media. In reaction (1.11), chloride ions in solution are oxidized, forming chlorine gas. In reaction (1.12), an iron metal electrode is dissolved, forming ferrous ions that go into solution. Reaction (1.13) represents a reversible oxide formation on a silver electrode. As electrons are removed from the silver metal, Ag^+ ions are formed. These Ag^+ ions then combine with hydroxyl (OH^-) ions from solution, forming an oxide layer (Ag_2O) on the surface of the silver electrode. Note the transfer of charge that occurs. As electrons are transferred to the electrode and then the external electrical circuit, the silver electrode is oxidized ($Ag \rightarrow Ag^+$). Because hydroxyl ions associate with the silver ions, the silver oxide is electroneutral. However, since hydroxyl has been removed from the solution, there is a net movement of negative charge from the electrolyte (loss of hydroxyl) to the electrode (electrons transferred to the electrode and then to the electrical circuit). The loss of hydroxyl lowers the solution pH.

1.3. Reversible and irreversible Faradaic reactions

There are two limiting cases that may define the net rate of a Faradaic reaction (Delahay, 1965; Bard and Faulkner, 1980; Pletcher and Walsh, 1990). At one extreme, the reaction rate is under kinetic control; at the other extreme, the reaction rate is under mass transport control. For a given metal electrode and electrolyte, there is an electrical potential (voltage) called the equilibrium potential where no net current passes between the two phases. At electrical potentials sufficiently close to equilibrium, the reaction rate is under kinetic control. Under kinetic control, the rate of electron transfer at the interface is determined by the electrode potential, and is *not* limited by the rate at which reactant is delivered to the electrode surface (the reaction site). When the electrode potential is sufficiently far away from equilibrium, the reaction rate is under mass transport control. In this case, all reactant that is delivered to the surface reacts immediately, and the reaction rate is limited by the rate of delivery of reactant to the electrode surface.

Faradaic reactions are divided into reversible and irreversible reactions (Bard and Faulkner, 1980). The degree of reversibility depends on the relative rates of kinetics (elec-

tron transfer at the interface) and mass transport. A Faradaic reaction with very fast kinetics relative to the rate of mass transport is reversible. With fast kinetics, large currents occur with small potential excursions away from equilibrium. Since the electrochemical product does not move away from the surface extremely fast (relative to the kinetic rate), there is an effective storage of charge near the electrode surface, and if the direction of current is reversed then some product that has been recently formed may be reversed back into its initial (reactant) form.

In a Faradaic reaction with slow kinetics, large potential excursions away from equilibrium are required for significant currents to flow. In such a reaction, the potential must be forced very far from equilibrium before the mass transport rate limits the net reaction rate. In the lengthy time frame imposed by the slow electron transfer kinetics, chemical reactant is able to diffuse to the surface to support the kinetic rate, and product diffuses away quickly relative to the kinetic rate. Because product diffuses away, there is no effective storage of charge near the electrode surface, in contrast to reversible reactions. If the direction of current is reversed, product will not be reversed back into its initial (reactant) form, since it has diffused away within the slow time frame of the reaction kinetics. Irreversible products may include species that are soluble in the electrolyte (e.g. reaction (1.12)), precipitate in the electrolyte, or evolve as a gas (e.g. reactions (1.1), (1.9) and (1.11)). Irreversible Faradaic reactions result in a net change in the chemical environment, potentially creating chemical species that are damaging to tissue or the electrode. Thus, as a general principle, an objective of electrical stimulation design is to avoid irreversible Faradaic reactions.

1.4. The origin of electrode potentials and the three-electrode electrical model

An electrical potential, or voltage, is always defined between two points in space. During electrical stimulation, the potentials of *both* the working and counter electrodes may vary with respect to some third reference point. A third electrode whose potential does not change over time, the reference electrode, may be employed for making potential measurements. Potentials of the working electrode and counter electrode may then be given with respect to the reference electrode.

Electrochemical potential, also known as transformed chemical potential, is a parameter that defines the driving force for all chemical processes, and is the sum of a chemical potential term and an electrical potential term (Silbey and Alberty, 2001). For a metal and a solution of its own ions in contact to be in equilibrium, the electrochemical potential of an electron must be the same in each phase. When two isolated phases are brought into contact, electron transfer may occur if the electrochemical potentials are unequal. Upon transferring electrons, a potential difference develops between the phases that repels further transfer. When electrochemical equilibrium is achieved, there is no further transfer of electrons, and a difference in inner potentials $\Delta\phi$ exists between the two phases (the inner potential ϕ is the electrical potential inside the bulk of the phase). The difference in inner potentials between a metal phase and solution phase in contact, $\Delta\phi_{\text{metal–solution}}$, defines the electrode interfacial potential. It is an experimental limitation that a single interfacial potential cannot be measured. Whenever a measuring instrument is introduced, a new interface is created and one is unable to separate the effects of the two interfaces. Evaluation must be of a complete electrochemical cell, which is generally considered as two electrodes separated by an electrolyte. Thus, practically, potentials are measured as complete cell potentials between two electrodes, either from the working electrode to the counter electrode, or from the working electrode to the reference electrode.[1] A cell potential is the sum of two interfacial potentials (electrode 1 to electrolyte plus electrolyte to electrode 2), as well as any potential occurring across the electrolyte as current flows. In the absence of current, the cell potential between the working electrode and reference electrode is called the open-circuit potential, and is the sum of two equilibrium interfacial potentials from the working electrode to the electrolyte and from the electrolyte to the reference electrode.

Consider the electron transfer reaction between a metal electrode and a reduction/oxidation (redox) couple O and R in solution:

$$\mathrm{O} + n\mathrm{e}^- \leftrightarrow \mathrm{R} \tag{1.14}$$

where O is the oxidized species of the couple, R is the reduced species, and n is the number of electrons transferred.

If the concentrations of both O and R in solution are equal, then the electrical potential of the redox couple equilibrates at $E^{\Theta'}$, the formal potential. More generally, if the concentrations of O and R are unequal, the equilibrium potential or Nernst potential E_{eq} may be calculated by the Nernst equation (Bard and Faulkner, 1980; Silbey and Alberty, 2001):

$$E_{\text{eq}} = E^{\Theta'} + \left(\frac{RT}{nF}\right) \ln\left\{\frac{[\mathrm{O}]}{[\mathrm{R}]}\right\} \tag{1.15}$$

where [O] and [R] are concentrations in the bulk solution, R is the gas constant ~8.314 J/(mol K), T is the absolute temperature, and F is Faraday's constant ~96,485 C/mole of electrons.

The Nernst Eq. (1.15) relates the equilibrium electrode potential E_{eq} (the electrical potential of the working electrode with respect to any convenient reference electrode) to the bulk solution concentrations [O] and [R] when the system is in equilibrium. As the bulk concentration [O] increases or the

[1] In the electrochemistry literature, the term "electrode potential" is not defined consistently. Some authors define the electrode potential as the potential between an electrode and a reference electrode, and sometimes it is defined as the (immeasurable) interfacial potential. For clarity and accuracy, when the term "electrode potential" is used, it should be specified what this potential is with respect to, e.g. the electrolyte, a reference electrode, or another electrode.

bulk concentration [R] decreases, the equilibrium potential becomes more positive.

In a system containing only one redox couple that has fairly fast kinetics, the measured open-circuit potential equals the equilibrium potential of the redox couple. If the kinetics of the redox couple are slow, the open-circuit potential (an empirical parameter) may not quickly attain the equilibrium potential after a perturbation, and if other contaminating redox couples are present that affect the equilibrium state, the measured open-circuit potential does not readily correlate with any single redox equilibrium potential.

If one begins with a system that is in equilibrium and then forces the potential of an electrode away from its equilibrium value, for example, by connecting a current source between the working and counter electrodes, the electrode is said to become polarized. Polarization is measured by the overpotential η, which is the difference between an electrode's potential and its equilibrium potential (both measured with respect to some reference electrode):

$$\eta \equiv E - E_{eq} \tag{1.16}$$

The electrode interface model of Fig. 1(b) demonstrates the mechanisms of charge injection from an electrode; however, it neglects the equilibrium interfacial potential $\Delta\phi$ that exists across the interface at equilibrium. This is modeled as shown in Fig. 2(a). In addition to the electrode interface, the solution resistance R_S (alternatively referred to as the access resistance R_A or the Ohmic resistance R_Ω) that exists between two electrodes in solution is modeled. An electrical circuit model of a three-electrode system, including the working electrode, counter electrode and reference electrode immersed into an electrolyte, is shown in Fig. 2(b). The reference electrode is used for potential measurements and is not required to pass current for stimulation; a two-electrode system (working and counter electrodes) is sufficient for stimulation. As current is passed between the working and counter electrodes through the electrolytic solution, the interfacial potentials $V_{WE–solution}$ and $V_{CE–solution}$ will vary from their equilibrium values, i.e. there are overpotentials associated with both interfaces. Also, as current flows there is a voltage drop across the resistive solution equal to the product of current and solution resistance: $v = iR_S$. Thus, if current flows and there is a change in the measured potential $V_{WE–CE}$, this change may be from any of three sources: (1) an overpotential at the working electrode as the interfacial potential $V_{WE–solution}$ varies; (2) an overpotential at the counter electrode as the interfacial potential $V_{CE–solution}$ varies; and (3) the voltage drop iR_S in solution. In the two-electrode system, one may only measure $V_{WE–CE}$, and the individual components of the two overpotentials and iR_S cannot be resolved. A third (reference) electrode may be used for potential measurements. An ideal reference electrode has a Faradaic reaction with very fast kinetics, which appears in the electrical model as a very low resistance for the Faradaic impedance $Z_{Faradaic}$. In this case, no significant overpotential occurs at the reference electrode during current flow, and the interfacial potential $V_{RE–solution}$ is considered constant. Examples of common reference electrodes are the reversible hydrogen electrode (RHE), the saturated calomel electrode (SCE), and the silver/silver chloride electrode (Ives and Janz, 1961). In the three-electrode system, if current flows through the working and counter electrodes and a change is noted in the measured potential $V_{WE–RE}$, this change may be from either of two sources: (1) an overpotential at the working electrode as the interfacial potential $V_{WE–solution}$ varies; and (2) the voltage drop iR_S in solution. Unlike the two-electrode system, only one overpotential contributes to the measured potential change. Furthermore, the overpotential at the working electrode can be estimated using the process of correction. This involves estimating the value of the solution resistance between the working electrode interface and the reference electrode interface, called the uncorrected solution resistance R_U, and multiplying R_U by the measured current. This product $V_{corr} = iR_{U,estimated}$ is then subtracted from the measured $V_{WE–RE}$ to yield the two interfacial potentials

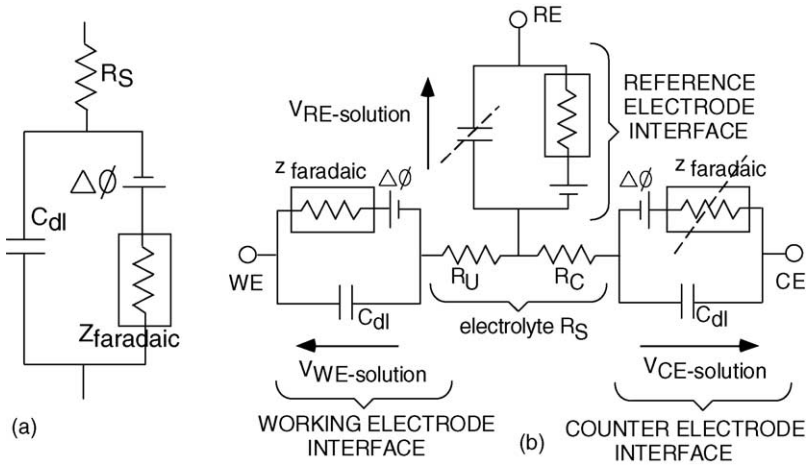

Fig. 2. Electrical circuit models: (a) single electrode/electrolyte interface; (b) three-electrode system. External access to the system is at three points labeled "WE", "CE" and "RE". If the counter electrode has a large surface area, it may be considered as strictly a capacitance as shown. A reference electrode with very low valued Faradaic resistance will maintain the interfacial potential $V_{RE–solution}$ constant.

$V_{WE–solution}$ and $V_{RE–solution}$. Since $V_{RE–solution}$ is constant, any change in $V_{WE–RE}$ is attributed to an overpotential at the working electrode interface.

1.5. Faradaic processes: quantitative description

Eq. (1.17), the current–overpotential equation (Bard and Faulkner, 1980), relates the overpotential to net current density through an electrode going into a Faradaic reaction, and defines the full characteristics of the Faradaic impedance:

$$i_{net} = i_0 \left\{ \frac{[O]_{(0,t)}}{[O]_\infty} \exp(-\alpha_c n f \eta) - \frac{[R]_{(0,t)}}{[R]_\infty} \exp((1-\alpha_c) n f \eta) \right\} \quad (1.17)$$

where i_{net} is the net Faradaic current across the electrode/electrolyte interface, i_0 is the exchange current density, $[O]_{(0,t)}$ and $[R]_{(0,t)}$ are concentrations at the electrode surface ($x = 0$) as a function of time, $[O]_\infty$ and $[R]_\infty$ are bulk concentrations, α_c is the cathodic transfer coefficient and equals ~0.5, n is the number of moles of electrons per mole of reactant oxidized (Eq. (1.14)), $f \equiv F/RT$, F is Faraday's constant ~96,485 C/mole of electrons, R is the gas constant ~8.314 J/(mol K), and T is the absolute temperature.

This equation relates the net current of a Faradaic reaction to three factors of interest: (1) the exchange current density i_0, which is a measure of the kinetic rate of the reaction; (2) an exponential function of the overpotential; and (3) the concentration of reactant at the electrode interface. The exponential dependence of Faradaic current on overpotential indicates that for a sufficiently small overpotential, there is little Faradaic current, i.e. for small potential excursions away from equilibrium, current flows primarily through the capacitive branch of Fig. 1, charging the electrode capacitance, not through the Faradaic branch. As more charge is delivered through an electrode interface, the electrode capacitance continues to charge, the overpotential increases, and the Faradaic current (proportional to $\exp(\eta)$) begins to be a significant fraction of the total injected current. For substantial cathodic overpotentials the left term of Eq. (1.17) dominates; for substantial anodic overpotentials the right term dominates.

Near equilibrium, the surface concentrations of O and R are approximately equal to the bulk concentrations. As more charge is delivered and the overpotential continues to increase, the surface concentration of reactant may decrease. The Faradaic current will then begin to level off, corresponding to the current becoming limited by mass transport of reactant. At the limiting currents $i_{L,c}$ (cathodic, for negative overpotentials) or $i_{L,a}$ (anodic, for positive overpotentials), the reactant concentration at the electrode surface approaches zero, and the terms $[O]_{(0,t)}/[O]_\infty$ or $[R]_{(0,t)}/[R]_\infty$ counteract the exponential terms in Eq. (1.17), dominating the solution for net reaction rate. In a mass transport limited reaction, the reactant concentration at the surface is considered zero, and the slope of the reactant concentration gradient between the electrode surface and the bulk electrolyte determines the rate of delivery of reactant, and thus the current.

The overpotential an electrode must be driven to before any given current will be achieved is highly dependent on the kinetics of the system, characterized by the exchange current density i_0. For a kinetically fast system with a large exchange current density, such as $i_0 = 10^{-3}$ A/cm^2, no significant overpotential may be achieved before a large current ensues. When the exchange current density is many orders of magnitude smaller such as $i_0 = 10^{-9}$ A/cm^2, a large overpotential must be applied before there is significant current.

As current is passed between a working electrode and counter electrode through an electrolyte, both the working and counter electrode's potentials move away from their equilibrium values, with one moving positive of its equilibrium value and the other moving negative of its equilibrium value. Total capacitance is proportional to area, with capacitance C_{dl} = (capacitance/area) × area. Capacitance/area is an intrinsic material property. Capacitance is defined as the ability to store charge, and is given by:

$$C_{dl} \equiv \frac{dq}{dV} \quad (1.18)$$

where q = charge and V = the electrode potential with respect to some reference electrode.

Thus, an electrode with a relatively large area and total capacity (as is often the case for a counter electrode) can store large amount of charge (dq) with a small overpotential (dV). During stimulation, the use of a large counter electrode keeps the potential of the counter electrode fairly constant during charge injection (near its equilibrium value), and there is little Faradaic current (Eq. (1.17)). Significant overpotentials may be realized at a small working electrode (small for purposes of spatial resolution during recording or stimulation). It is common to neglect the counter electrode in analysis, and while this is often a fair assumption it is not always the case.

1.6. Ideally polarizable electrodes and ideally non-polarizable electrodes

Two limiting cases for the description of an electrode are the ideally polarizable electrode, and the ideally non-polarizable electrode (Delahay, 1965; Gileadi et al., 1975; Bard and Faulkner, 1980). The ideally polarizable electrode corresponds to an electrode for which the $Z_{Faradaic}$ element has infinite resistance (i.e. this element is absent). Such an electrode is modeled as a pure capacitor, with $C_{dl} = dq/dV$ (Eq. (1.18)), in series with the solution resistance. In an ideally polarizable electrode, no electron transfer occurs across the electrode/electrolyte interface at any potential when current is passed; rather all current is through capacitive action. No sustained current flow is required to support a large voltage change across the electrode interface. An ideally polarizable electrode is not used as a reference electrode, since the electrode potential is easily perturbed away from the equilibrium potential. A highly polarizable

(real) electrode is one that can accommodate a large amount of injected charge on the double layer prior to initiating Faradaic reactions, corresponding to a relatively small exchange current density, e.g. $i_0 = 10^{-9}$ A/cm^2.

The ideally non-polarizable electrode corresponds to an electrode for which the $Z_{Faradaic}$ element has zero resistance; thus, only the solution resistance appears in the model. In the ideally non-polarizable electrode current flows readily in Faradaic reactions and injected charge is accommodated by these reactions. No change in voltage across the interface occurs upon the passage of current. This is the desired situation for a reference electrode, so that the electrode potential remains near equilibrium even upon current flow. A highly non-polarizable (real) electrode, for which the $Z_{Faradaic}$ element has very small resistance, has a relatively large exchange current density, e.g. $i_0 = 10^{-3}$ A/cm^2. Most real electrode interfaces are modeled by a C_{dl} in parallel with a finite $Z_{Faradaic}$, together in series with the solution resistance (Fig. 2(a)).

Consider a metal electrode consisting of a silver wire placed inside the body, with a solution of silver ions between the wire and ECF, supporting the reaction $Ag^+ + e^- \leftrightarrow Ag$. This is an example of an electrode of the first kind, which is defined as a metal electrode directly immersed into an electrolyte of ions of the metal's salt. As the concentration of silver ions [Ag^+] decreases, the resistance of the interface increases. At very low silver ion concentrations, the Faradaic impedance $Z_{Faradaic}$ becomes very large, and the interface model shown in Fig. 2(a) reduces to a solution resistance R_S in series with the capacitance C_{dl}. Such an electrode is an ideally polarizable electrode. At very high silver concentrations, the Faradaic impedance approaches zero and the interface model of Fig. 2(a) reduces to a solution resistance in series with the Faradaic impedance $Z_{Faradaic}$, which is approximated by the solution resistance only. Such an electrode is an ideally non-polarizable electrode. The example of a silver electrode placed in direct contact with the ECF, acting as an electrode of the first kind, is impractical. Silver is toxic, silver ions are not innate in the body, and any added silver ions may diffuse away. The silver wire electrode is a highly polarizable electrode since the innate silver concentration is very low and the Faradaic reaction consumes little charge; thus, this configuration is not usable as a reference electrode. The equilibrium potential, given by a derivation of the Nernst equation

$$E_{eq} = E^{\Theta} + (RT/nF)\ln[Ag^+] = (59\,\text{mV/decade})\log[Ag^+]$$

at 25 °C, is poorly defined due to the low silver ion concentration. A solution to these problems is to use an electrode of the second kind, which is defined as a metal coated with a sparingly soluble metal salt. The common silver/silver chloride (Ag/AgCl) electrode, described by reactions (1.8a) and (1.8b), is such an electrode. This consists of a silver electrode covered with silver chloride, which is then put in contact with the body. The Ag/AgCl electrode acts as a highly non-polarizable electrode. The equilibrium potential $E_{eq} = E^{\Theta} + 59\log[Ag^+]$ can be combined with the definition of the silver chloride solubility constant, $K_S \equiv [Ag^+][Cl^-] \sim 10^{-10}$ M^2, to yield $E_{eq} = E^{\Theta} + 59\log[K_S/Cl^-] = E^{\Theta} + 59\log K_S - 59\log[Cl^-] = E^{\Theta'} - 59\log[Cl^-]$. The equilibrium potential of this electrode of the second kind is seen to be dependent on the finite chloride concentration rather than any minimal silver concentration, and is well defined for use as a reference electrode.

2. Charge injection across the electrode/electrolyte interface during electrical stimulation

2.1. Charge injection during pulsing: interaction of capacitive and Faradaic mechanisms

As illustrated in Fig. 1, there are two primary mechanisms of charge injection from a metal electrode into an electrolyte. The first consists of charging and discharging the double layer capacitance, causing a redistribution of charge in the electrolyte but no electron transfer from the electrode to the electrolyte. C_{dl} for a metal in aqueous solution has values on the order of 10–20 μF/cm^2 of real area (geometric area multiplied by the roughness factor). For a small enough total injected charge, all charge injection is by charging and discharging of the double layer. Above some injected charge density, a second mechanism occurs consisting of Faradaic reactions where electrons are transferred between the electrode and electrolyte, thus changing the chemical composition in the electrolyte by reduction or oxidation reactions. Fig. 1 illustrates a single Faradaic impedance representing the electron transfer reaction $O + ne^- \leftrightarrow R$. Generally there may be more than one Faradaic reaction possible, which is modeled by several branches of $Z_{Faradaic}$ (one for each reaction), all in parallel with the double layer capacitance. The current–overpotential Eq. (1.17), and Fick's first and second laws for diffusion, give the complete description of processes occurring for any Faradaic reaction.

In addition to the double layer capacitance, some metals have the property of pseudocapacity (Gileadi et al., 1975), where a Faradaic electron transfer occurs, but because the product remains bound to the electrode surface, the reactant may be recovered (the reaction may be reversed) if the direction of current is reversed. Although electron transfer occurs, in terms of the electrical model of Fig. 1 the pseudocapacitance is better modeled as a capacitor, since it is a charge storage (not dissipative) process. Platinum is commonly used for stimulating electrodes, as it has a pseudocapacity (by reaction (1.6)) of 210 μC/cm^2 real area (Rand and Woods, 1971), or equivalently 294 μC/cm^2 geometric area using a roughness factor of 1.4.[2]

[2] The relationship between capacitance and stored charge is given by Eq. (2.3). A 1 V potential excursion applied to a double layer capacitance of 20 μF/cm^2 yields 20 μC/cm^2 stored charge, which is an order of magnitude lower than the total charge storage available from platinum pseudocapacitance.

It is a general principle when designing electrical stimulation systems that one should avoid onset of irreversible Faradaic processes which may potentially create damaging chemical species, and keep the injected charge at a low enough level where it may be accommodated strictly by reversible charge injection processes. Unfortunately, this is not always possible, because a larger injected charge may be required to cause the desired effect (e.g. initiating action potentials). Reversible processes include charging and discharging of the double layer capacitance, reversible Faradaic processes involving products that remain bound to the surface such as plating of hydrogen atoms on platinum (reaction (1.6)) or the reversible formation and reduction of a surface oxide (reactions (1.4) and (1.5a)–(1.5c)), and reversible Faradaic processes where the solution phase product remains near the electrode due to mass diffusion limitations.

The net current passed by an electrode, modeled as shown in Fig. 1, is the sum of currents through the two parallel branches. The total current through the electrode is given by:

$$i_{\text{total}} = i_{\text{c}} + i_{\text{f}} \tag{2.1}$$

where i_{c} is the current through the capacitance and i_{f} is the current through the Faradaic element.

The current through the Faradaic element is given by the current–overpotential equation (1.17). The current through the capacitance is given by Eq. (2.2):

$$i_{\text{c}} = C_{\text{dl}} \frac{\text{d}v}{\text{d}t} = C_{\text{dl}} \frac{\text{d}\eta}{\text{d}t} \tag{2.2}$$

The capacitive current depends upon the rate of potential change, but not the absolute value of the potential. The Faradaic current, however, is exponentially dependent upon the overpotential, or departure from the equilibrium potential. Thus, as an electrode is driven away from its equilibrium potential, essentially all charge initially flows through the capacitive branch since the overpotential is small near equilibrium. As the overpotential increases, the Faradaic branch begins to conduct a relatively larger fraction of the injected current. When the overpotential becomes great enough, the Faradaic impedance becomes small enough that the Faradaic current equals the injected current. At this point, the Faradaic process of reduction or oxidation conducts all injected charge, and the potential of the electrode does not change, corresponding to the capacitor not charging any further.

In terms of charge going into the different processes, the charge on the double layer capacitance is proportional to the voltage across the capacitance:

$$q_{\text{c}} = C_{\text{dl}}\, \Delta V \tag{2.3}$$

Thus, if the electrode potential does not change in time, neither does the stored charge. The charge into Faradaic processes, however, does continue to flow for any non-zero overpotential. The Faradaic charge is the integration of Faradaic current over time, which by Eq. (1.17) is proportional to an exponential of the overpotential integrated over time:

$$q_{\text{f}} = \int i_{\text{f}}\, \text{d}t \propto \int \exp(\eta)\, \text{d}t \tag{2.4}$$

The charge delivered into Faradaic reactions is directly proportional to the mass of Faradaic reaction product formed, which may be potentially damaging to the tissue being stimulated or the electrode.

2.2. Methods of controlling charge delivery during pulsing

Charge injection from an electrode into an electrolyte (e.g. extracellular fluid) is commonly controlled by one of three methods. In the current-controlled (also called galvanostatic) method, a current source is attached between the working and counter electrodes and a user-defined current is passed. In the voltage-controlled (also called potentiostatic) method, current is driven between the working electrode and counter electrode as required to control the working electrode potential with respect to a third (reference) electrode. This may be used for electrochemical measurements of certain neurotransmitters (reviewed by Michael and Wightman, 1999). This method is most often not used for stimulation, and is not discussed further in this review. In the third method, $V_{\text{WE–CE}}$ control, a voltage source is applied between the working and counter electrodes. While this is the simplest method to implement, neither the potential of the working electrode nor the potential of the counter electrode (with respect to a third reference electrode) are controlled; only the net potential between the working and counter electrodes is controlled.

2.3. Charge delivery by current control

The current-controlled method is commonly used for functional electrical stimulation of excitable tissue. This typically takes the form of pulsing. In monophasic pulsing, a constant current is passed for a period of time (generally on the order of tens to hundreds of microseconds), and then the external stimulator circuit is open circuited (it is effectively electrically removed from the electrodes) until the next pulse. In biphasic pulsing, a constant current is passed in one direction, then the direction of current is reversed, and then the circuit is open circuited until the next pulse. In biphasic pulsing the first phase, or stimulating phase, is used to elicit the desired physiological effect such as initiation of an action potential, and the second phase, or reversal phase, is used to reverse electrochemical processes occurring during the stimulating pulse. It is common to use a cathodic pulse as the stimulating phase (the working electrode is driven negative with respect to its pre-pulse potential), followed by an anodic reversal phase (the working electrode is driven positive), although anodic pulsing may also be used for stimulation (discussed in Section 4). Fig. 3 illustrates definitions of the key parameters in pulsing. The frequency of stimulation is the inverse of the period, or time between pulses. The interpulse

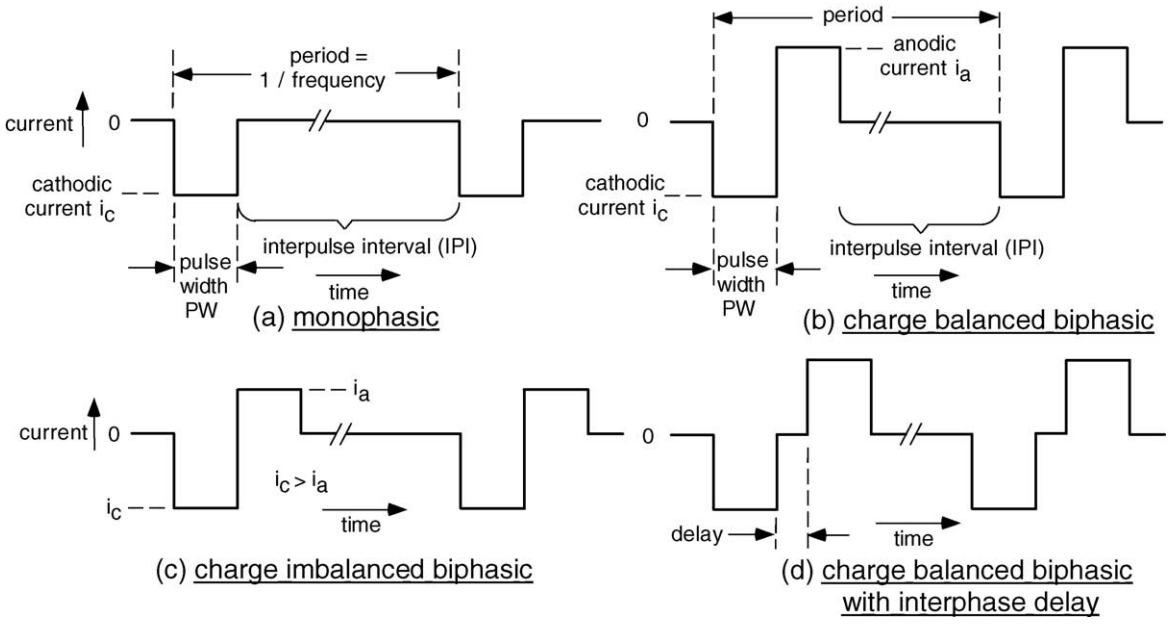

Fig. 3. Common pulse types and parameters.

interval is the period of time between pulses. Fig. 3(b) illustrates charge-balanced biphasic pulsing, where the charge in the stimulation phase equals the charge in the reversal phase. Fig. 3(c) illustrates charge-imbalanced biphasic pulsing (detailed in Section 4) where there are two phases, but the reversal phase has less charge than the stimulating phase. Fig. 3(d) illustrates the use of an interphase delay, where an open circuit is introduced between the stimulating and reversal phases.

Upon application of a cathodic current pulse to an electrode that starts at a potential close to the equilibrium potential, the term $\exp(\eta)$ is small and initially little charge goes into any Faradaic reactions, thus the initial charge delivery goes into charging the double layer capacitance. As charge goes onto the double layer, the electrode potential moves away from equilibrium (an overpotential η develops), and the Faradaic reaction $O + ne^- \rightarrow R$ starts to consume charge, with net current density proportional to $\exp(\eta)$. The total injected current then goes into both capacitive current i_c, causing the electrode to continue to charge negatively, and Faradaic current i_f. The Faradaic reaction will consume reactant O near the surface, and the concentration $[O]_{(0,t)}$ drops. Once the concentration $[O]_{(0,t)}$ becomes zero, the Faradaic reaction is mass transport limited, and the current into this reaction no longer increases as $\exp(\eta)$. A portion of the injected charge goes into capacitive current, causing the double layer to continue to charge to more negative potentials. At sufficiently negative potentials, another Faradaic reaction with a lower exchange current density (thus more irreversible) than the first may start. In the case where this second reaction is the reduction of water, the reaction will not become mass transport limited (water at 55.5 M will support substantial current), and an electrode potential will be reached where the non-mass transport limited reduction of water accepts all further injected charge. The water window is a potential range that is defined by the reduction of water, forming hydrogen gas, in the negative direction, and the oxidation of water, forming oxygen, in the positive direction. Because water does not become mass transport limited in an aqueous solution, the potentials where water is reduced and oxidized form lower and upper limits respectively for electrode potentials that may be attained, and any electrode driven to large enough potentials in water will evolve either hydrogen gas or oxygen gas. Upon reaching either of these limits, all further charge injection is accommodated by the reduction or oxidation of water.

2.4. Pulse train response during current control

Based on the simple electrical model of Fig. 1, one may predict different characteristics in the potential waveforms resulting from monophasic pulsing, charge-balanced biphasic pulsing, and charge-imbalanced biphasic pulsing. Consider what occurs when an electrode, starting from the open-circuit potential, is pulsed with a single cathodic pulse and then left open circuit (illustrated in Fig. 4(a), pulse 1). Upon pulsing the electrode charges, with injected charge being stored reversibly on the double layer capacitance, causing the electrode potential to move negative. As the potential continues to move negative, charge begins to be delivered into Faradaic currents (whose magnitude are an exponential function of the overpotential). At the end of the pulse when the external circuit is opened, charge on the double layer capacitance continues to discharge through Faradaic reactions. This causes the electrode potential to move positive during discharge, and as the electrode discharges (i.e. the overpotential decreases) the Faradaic current decreases, resulting in an exponential discharge of the electrode. Given a long enough time, the

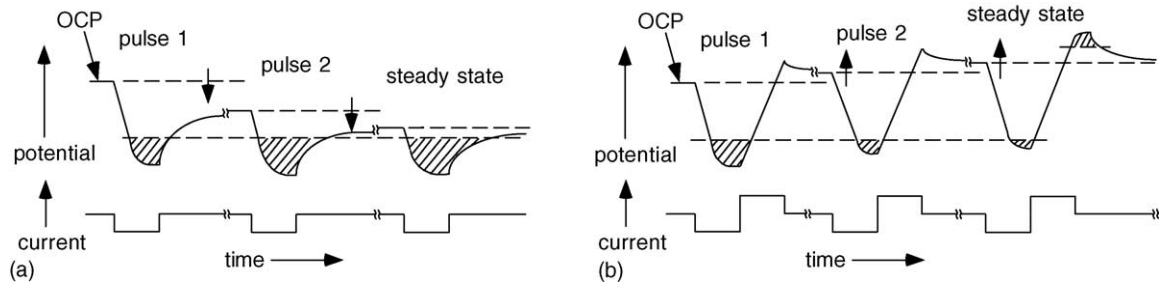

Fig. 4. Electrode potentials in response to monophasic and charge-balanced biphasic pulse trains. (a) Ratcheting of potential during monophasic cathodic pulsing. The pre-pulse potential of successive pulses moves negative until all injected charge goes into irreversible processes. (b) Ratcheting during charge-balanced cathodic first biphasic pulsing. The pre-pulse potential of successive pulses moves positive until the same amount of charge is lost irreversibly during the cathodic and anodic phases. Shaded areas represent periods of irreversible reactions.

electrode potential will approach the open-circuit potential. However, if the electrode is pulsed with a train whose period is short with respect to the time constant for discharge (as may occur with neural stimulation, with a period of perhaps 20 ms), i.e. if a second cathodic pulse arrives before the electrode has completely discharged, then the potential at the start of the second pulse (the pre-pulse potential) is more negative than the pre-pulse potential of the first pulse (which is the open-circuit potential). Because the potential during the second pulse begins at a more negative potential than the first, a smaller fraction of the injected charge goes into reversible charging of the double layer capacitance. The Faradaic reactions begin accepting significant charge at an earlier time than in the first pulse, and there is more charge delivered to irreversible reactions during the second pulse than during the first as the overall potential range traversed is more negative during the second pulse (Fig. 4(a), pulse 2). Upon going to open circuit after the second pulse, the electrode discharges through Faradaic reactions. Because the potential at the end of the second current pulse is more negative than the potential at the end of the first current pulse, the potential range during discharge between pulses 2 and 3 is also more negative than between pulses 1 and 2, and likewise the pre-pulse potential of pulse 3 is more negative than the pre-pulse potential of pulse 2. This "ratcheting" of the electrode potential continues until the following condition is met:

$$\text{unrecoverable charge}\,(Q_{\text{ur}})\,\text{per pulse} = \text{injected charge}\,(Q_{\text{inj}})\,\text{per pulse} \tag{2.5}$$

i.e. all injected charge goes into irreversible Faradaic reactions that occur either during the pulse or during the open circuit interpulse interval period. Charge delivered into irreversible processes is defined as unrecoverable charge Q_{ur}. Once condition (2.5) is met, the pulsing is in the steady state, and the potential excursions repeat themselves with each pulse cycle.

Next, consider the electrode response when a charge-balanced stimulation protocol is used; cathodic then anodic, followed by open circuit. The electrode begins from open-circuit potential. Upon applying the first cathodic pulse, the double layer reversibly charges, and then the electrode may begin to transfer charge into Faradaic reactions as the potential moves negative. The anodic pulse then causes the electrode potential to move back positive (illustrated in Fig. 4(b), pulse 1). Unlike the exponential decay during the monophasic pulsing, the electrode potential now changes according to the anodic current and the double layer capacitance, and there is reversal of charge from the double layer. Because not all of the injected charge during the cathodic pulse went into charging of the double layer, only some fraction of the injected cathodic charge is required in the anodic phase to bring the electrode potential back to the pre-pulse value. Since the anodic pulse is balanced with the cathodic pulse, the electrode potential at the end of the anodic phase of pulse 1 is positive of the pre-pulse potential of pulse 1 (the open-circuit potential). During the anodic phase and during the open circuit following the anodic phase, if the potential becomes sufficiently positive, anodic Faradaic reactions such as electrode corrosion may occur. During the open-circuit period, the electrode discharges exponentially through anodic Faradaic reactions back towards the open-circuit potential, moving negative with time. By the beginning of pulse 2 the potential is still positive of the pre-pulse potential for pulse 1 (the open-circuit potential). Thus, as long as any charge is lost irreversibly during the cathodic phase, the potential at the end of the charge-balanced anodic phase will be positive of the pre-pulse potential, and a ratcheting effect is seen. Unlike the monophasic case, the ratcheting of the electrode pre-pulse potential is now in a positive direction. Steady state occurs when one of the two following conditions is met:

(1) There are no irreversible Faradaic reactions during either the cathodic or anodic phases, and the electrode simply charges and then discharges the double layer (the potential waveform appears as a sawtooth):

$$Q_{\text{ur,cathodic}} = Q_{\text{ur,anodic}} = 0 \tag{2.6}$$

(2) The same amount of charge is lost irreversibly during the cathodic phase and the anodic phase:

$$Q_{\text{ur,cathodic}} = Q_{\text{ur,anodic}} \neq 0 \tag{2.7}$$

If irreversible processes do occur, for cathodic first charge-balanced biphasic pulsing, the electrode potential will move

positive of the open-circuit potential, and during steady-state continuous pulsing there is an equal amount of unrecoverable charge delivered into cathodic and anodic irreversible processes.

Finally, consider the electrode response when a charge-imbalanced stimulation protocol is used (not illustrated). The electrode begins from open-circuit potential. The response to the first cathodic pulse is the same as with the monophasic or charge-balanced biphasic waveforms. The anodic phase then causes the electrode potential to move back positive, but since there is less charge in the anodic phase than cathodic, the electrode potential does not move as far positive as it did with the charge-balanced biphasic waveform. The potential at the end of the anodic phase will be closer to the open-circuit potential than during charge-balanced pulsing. The maximum positive potential will be less when using the charge-imbalanced waveform than when using the charge-balanced waveform. This has the advantage that charge delivered into anodic Faradaic processes such as metal corrosion is reduced with respect to charge-balanced stimulation. The pre-pulse potential will move under factors as explained for the monophasic and charge-balanced biphasic waveforms until the following condition is met:

The net imbalance in injected charge is equal to the net difference in cathodic and anodic unrecoverable charge:

$$(Q_{\text{inj,cathodic}} - Q_{\text{inj,anodic}}) \equiv Q_{\text{imbal}} = Q_{\text{ur,cathodic}} - Q_{\text{ur,anodic}} \quad (2.8)$$

During charge-imbalanced stimulation, the shift in pre-pulse potential may be either positive or negative of the open-circuit potential depending on the amount of imbalance.

Based on these considerations, monophasic pulsing causes the greatest shift of the electrode potential during pulsing away from the equilibrium potential, thus causes the most accumulation of unrecoverable charge (corresponding to products of irreversible Faradaic reactions) of the three protocol types (monophasic, charge-balanced biphasic, charge-imbalanced biphasic). Furthermore, since during monophasic pulsing the electrode potential is not brought back towards the equilibrium potential by an anodic phase, there is accumulation of unrecoverable charge during the open circuit interpulse interval.

2.5. Electrochemical reversal

The purpose of the reversal phase during biphasic stimulation is to reverse the direction of electrochemical processes that occurred during the stimulating phase, minimizing unrecoverable charge. A reversible process is one where the reactants are reformed from the products upon reversing the direction of current. Upon delivering current in the stimulation phase and then reversing the direction of current, charge on the electrode capacitance will discharge, returning the electrode potential towards its pre-pulse value. If only double layer charging occurred, then upon passing an amount of charge in the reversal phase equal to the charge delivered in the stimulation phase (a charge-balanced protocol), the electrode potential will return precisely to its pre-pulse potential by the end of the reversal phase and the potential curve will be a simple sawtooth as shown in Fig. 5(a) (corrected for solution resistance). If reversible Faradaic reactions occur during the stimulation phase, then charge in the reversal or secondary phase may go into reversing these reactions. Fig. 5(b) illustrates an example reversible Faradaic process, in this case charging of the pseudocapacitance (reduction of protons and plating of monatomic hydrogen onto the metal electrode surface) as may occur on platinum. During reversal the plated hydrogen is oxidized back to protons. Because the electrochemical process occurring during the reversal phase is the exact opposite of that occurring during the stimulation phase, there is zero net accumulation of electrochemical species. Reversible Faradaic reactions include adsorption processes as in Fig. 5(b), as well as processes where the solution phase product remains near the electrode due to mass diffusion limitations. If irreversible Faradaic reactions occur, upon passing current in the reverse direction, reversal of electrochemical product does not occur as the product is no longer available for reversal (it has diffused away). An example shown in Fig. 5(c) is the formation of hydrogen gas after a monolayer of hydrogen atoms has been adsorbed onto the platinum surface. In the case where a Faradaic reaction has occurred during the stimulation phase, the potential waveform during the stimulation phase is not linear, but displays a slope inflection as Faradaic processes consume charge (this is charge that does *not* charge the capacitance, thus does not change the electrode potential). When an equal amount of charge is then passed in the reversal phase, the electrode potential goes positive of the pre-pulse potential. To return the electrode potential exactly to its pre-pulse value would require that the charge in the reversal phase be equal to only the amount of charge that went onto the capacitance during the stimulation phase (a charge-imbalanced waveform).

The use of biphasic stimulation (either charge-balanced or charge-imbalanced) moves the electrode potential out of the most negative ranges immediately after stimulation. In comparison (as shown in Fig. 4), the monophasic stimulation protocol allows the electrode potential to remain relatively negative during the interpulse interval, and during this time Faradaic reduction reactions may continue. In the presence of oxygen, these reactions may include reduction of oxygen and formation of reactive oxygen species, which have been implicated in tissue damage (reviewed by Halliwell, 1992; Stohs, 1995; Hemnani and Parihar, 1998; Imlay, 2003; Bergamini et al., 2004). The charge-imbalanced waveform has the added advantage that the electrode potential at the end of the anodic pulse is less positive than with charge-balanced biphasic pulsing, thus less charge goes into irreversible oxidation reactions such as corrosion when using the charge-imbalanced protocol. Charge-imbalanced biphasic waveforms provide a method to reduce unrecoverable charge in the cathodic

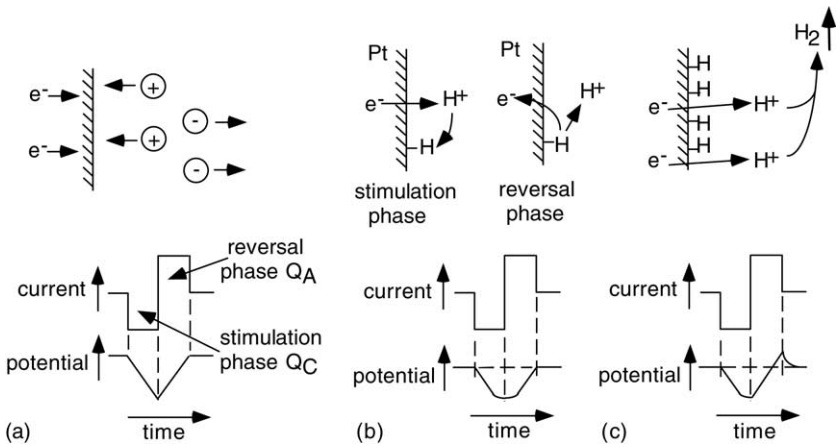

Fig. 5. Electrochemical processes and potential waveforms during charge-balanced stimulation: (a) capacitive charging only; (b) reversible hydrogen plating; (c) irreversible hydrogen evolution.

direction (with respect to monophasic stimulation) and in the anodic direction (with respect to charge-balanced biphasic stimulation), thus are an attractive solution to minimizing damage to either the stimulated tissue or the metal electrode.

2.6. Charge delivery by a voltage source between the working electrode and counter electrode

An alternative form of charge injection involves the direct connection of a voltage source between the working and counter electrodes. Fig. 6 compares the current, working electrode to reference electrode voltage ($V_{WE–RE}$), and working electrode to counter electrode voltage ($V_{WE–CE}$) waveforms during monophasic pulsing under current control versus $V_{WE–CE}$ control. The $V_{WE–RE}$ waveforms represent the working electrode interfacial potentials and do not imply that a reference electrode is required for either control scheme.

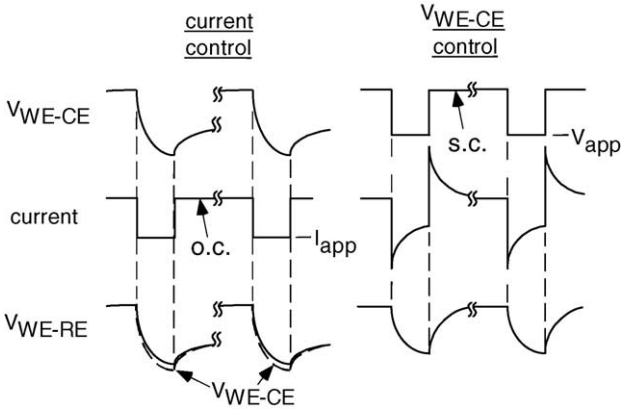

Fig. 6. Steady-state voltage and current waveforms using current control and $V_{WE–CE}$ control. Note the rapid discharge of the working electrode during the short circuit interpulse interval of $V_{WE–CE}$ control relative to the open circuit interpulse interval of current control. S.C. = short circuit; O.C. = open circuit; I_{app} = applied current; V_{app} = applied voltage.

Upon applying a voltage pulse with amplitude V_{app} between the working electrode and counter electrode in $V_{WE–CE}$ control, the current is at its maximum value at the beginning of the pulse as the double layer capacitances of the two electrodes charge and the current is predominantly capacitive. Given a long duration pulse, the current will asymptotically approach a value where V_{app} maintains a steady-state Faradaic current, with current density given by Eq. (1.17). Fig. 6 illustrates the steady-state waveforms when using an exhausting circuit (Donaldson and Donaldson, 1986a, 1986b), where at the end of the monophasic voltage pulse the working and counter electrodes are shorted together, causing the charge on the working electrode capacitance to rapidly discharge, and the working electrode potential to attain the counter electrode potential. If the counter electrode is sufficiently large, its potential will not be notably perturbed away from its equilibrium potential during pulsing, and upon shorting the working electrode to the counter electrode, the working electrode potential will be brought back to the counter electrode equilibrium potential. Donaldson and Donaldson showed that during cathodic monophasic pulsing of real electrodes with an exhausting scheme, the potentials of both the working electrode and counter electrode moved positive in response to a continuous train, increasing the risk of oxidizing reactions such as corrosion. The discharge of the working electrode is relatively rapid during $V_{WE–CE}$ control with an exhausting circuit, as the working electrode is directly shorted to the counter electrode. This is contrasted by the relatively slow discharge using monophasic current control as shown in Fig. 6, with an open circuit during the interpulse interval. During the open-circuit period, the working electrode capacitance discharges through Faradaic reactions at the working electrode interface. This leads to a greater accumulation of unrecoverable charge during the open circuit interpulse interval (current control) than with the short circuit interpulse interval ($V_{WE–CE}$ control). However, in current control, appropriate biphasic pulsing waveforms (Fig. 3) can promote rapid electrode discharge.

Advantages of the V_{WE-CE} control scheme over the current control scheme include: (1) the circuitry is simpler (it may be a battery and an electronic switch); and (2) unrecoverable charge accumulation is lower during the interpulse interval than it would be with monophasic current control. Disadvantages of the V_{WE-CE} control scheme include: (1) maximum stimulation of excitable tissue occurs only at the beginning of the pulse when current is maximum, and stimulation efficiency decreases throughout the pulse as current decreases, whereas with current control the current is constant throughout the pulse; (2) an increase in resistance anywhere in the electrical conduction path will cause an additional voltage drop, decreasing the current and potentially causing it to be insufficient for stimulation, whereas with current control the current is constant (assuming the required voltage is within the range of the stimulator); and (3) neither the current driven nor the charge injected are under direct control using voltage control (Weinman and Mahler, 1964). Because the level of neuronal membrane depolarization is related to the applied current, these factors result in a reduction in reproducibility between experiments, as well as between clinical implants, during V_{WE-CE} control. Moreover, because tissue properties can change over time, stimulation efficacy may change when using V_{WE-CE} control.

3. Materials used as electrodes for charge injection and reversible charge storage capacity

The ideal material for use as a stimulating electrode satisfies the following requirements. (1) The passive (unstimulated) material must be biocompatible, so it should not induce a toxic or necrotic response in the adjacent tissue, nor an excessive foreign body or immune response. (2) The material must be mechanically acceptable for the application. It must maintain mechanical integrity given the intended tissue, surgical procedure and duration of use. The material must not buckle if it is to pass through the meninges. If a device is to be used chronically, it must be flexible enough to withstand any small movement between the device and tissue following implantation. (3) The complete device must be efficacious. This requires that sufficient charge can be injected with the chosen material and electrode area to elicit action potentials. The required charge is quantified by the charge–duration curve, discussed in Section 4. (4) During electrical stimulation, Faradaic reactions should not occur at levels that are toxic to the surrounding tissue. The level of reaction product that is tolerated may be significantly higher for acute stimulation than chronic stimulation. (5) During electrical stimulation, Faradaic corrosion reactions should not occur at levels that will cause premature failure of the electrode. This again depends greatly on the intended duration of use. During acute stimulation corrosion is rarely a concern, whereas a device that is intended for a 30-year implant must have a very low corrosion rate. (6) The material characteristics must be acceptably stable for the duration of the implant. For a chronic electrode, the device electrical impedance must be stable. The conducting and insulating properties of all materials must remain intact.

Dymond et al. (1970) tested the toxicity of several metals implanted into the cat cerebral cortex for 2 months. Materials were deemed toxic if the reaction to the implanted metal was significantly greater than the reaction to a puncture made from the same metal that was immediately withdrawn (Table 1). Stensaas and Stensaas (1978) reported on the biocompatibility of several materials implanted passively into the rabbit cerebral cortex (Table 1). Materials were classified into one of three categories depending upon changes occurring at the implant/cortex interface. (1) *Non-reactive*: for these materials, little or no gliosis occurred, and normal CNS tissue with synapses was observed within 5 μm of the interface. (2) *Reactive*: multinucleate giant cells and a thin layer (10 μm) of connective tissue surrounded the implant. Outside of this was a zone of astrocytosis. Normal CNS tissue was observed within 50 μm of the implant. (3) *Toxic*: these materials are separated from the cortical tissue by a capsule of cellular connective tissue and a surrounding zone of astrocytosis. Loeb et al. (1977) studied the histological response to materials used by the microelectronics industry implanted chronically in the subdural space of cats, and found reactions to be quite dependent on specific material formulations and surface preparations.

Platinum has been demonstrated as biocompatible for use in an epiretinal array (Majji et al., 1999) and in cochlear implants (Chouard and Pialoux, 1995). Both titanium and ceramic (Chouard and Pialoux, 1995) and platinum–iridium wire (Niparko et al., 1989) have been shown as biocompatible in cochlear implants. Babb and Kupfer (1984) have shown stainless steel and nickel–chromium (Nichrome) to be nontoxic. Copper and silver are unacceptable as stimulating electrodes, as these metals cause tissue necrosis even in the absence of current (Fisher et al., 1961; Dymond et al., 1970; Sawyer and Srinivasan, 1974; Stensaas and Stensaas, 1978; Babb and Kupfer, 1984). Nickel–titanium shape memory alloys have good biocompatibility response (Ryhanen et al., 1998), up to a nickel content of 50% (Bogdanski et al., 2002).

The first intracortical electrodes consisted of single site conductive microelectrodes made of material stiff enough to penetrate the meninges, either an insulated metallic wire or a glass pipette filled with conductive electrolyte. Advances in materials science and microelectronics technology have allowed the development of multiple site electrodes built onto a single substrate, using planar photolithographic and silicon micromachining technologies. Such devices have been made from silicon (Jones et al., 1992; Hoogerwerf and Wise, 1994), and polyimide (Rousche et al., 2001). In further advancements, bioactive components have been added to the electrode to direct neurite growth toward the electrode, minimizing the distance between the electrode and stimulated tissue (Kennedy, 1989; Kennedy and Bakay, 1998; Kennedy et al., 1999).

Table 1
Classification of material biocompatibility

	Classification by Dymond et al.	Classification by Stensaas and Stensaas	Other references
Conductors			
Aluminum		Non-reactive	
Cobalt		Toxic	
Copper		Toxic	Toxic (Fisher et al., 1961; Sawyer and Srinivasan, 1974; Babb and Kupfer, 1984)
Gold	Non-toxic	Non-reactive	
Gold–nickel–chromium	Non-toxic		
Gold–palladium–rhodium	Non-toxic		
Iron		Toxic	
Molybdenum		Reactive	
Nickel–chromium (Nichrome)		Reactive	Non-toxic (Babb and Kupfer, 1984)
Nickel–chromium–molybdenum	Non-toxic		
Nickel–titanium (Nitinol)			Biocompatible (Ryhanen et al., 1998; Bogdanski et al., 2002)
Platinum	Non-toxic	Non-reactive	Biocompatible (Chouard and Pialoux, 1995; Majji et al., 1999)
Platinum–iridium	Non-toxic		Biocompatible (Niparko et al., 1989)
Platinum–nickel	Non-toxic		
Platinum–rhodium	Non-toxic		
Platinum–tungsten	Non-toxic		
Platinized platinum (Pt black)	Non-toxic		
Rhenium	Non-toxic		
Silver	Toxic	Toxic	Toxic (Fisher et al., 1961; Sawyer and Srinivasan, 1974; Babb and Kupfer, 1984)
Stainless steel	Non-toxic		Non-toxic (Babb and Kupfer, 1984)
Tantalum		Reactive	
Titanium			Biocompatible (Chouard and Pialoux, 1995)
Tungsten		Non-reactive	
Insulators			
Alumina ceramic		Non-reactive	Biocompatible (Chouard and Pialoux, 1995)
Araldite (epoxy plastic resin)		Reactive	
Polyethylene		Non-reactive	
Polyimide			Biocompatible (Stieglitz and Meyer, 1999)
Polypropylene		Non-reactive	
Silastic RTV		Toxic	
Silicon dioxide (Pyrex)		Reactive	
Teflon TFE (high purity)		Non-reactive	
Teflon TFE (shrinkable)		Reactive	
Titanium dioxide		Reactive	
Semiconductors			
Germanium		Toxic	
Silicon		Non-reactive	Biocompatible (Schmidt et al., 1993; Hoogerwerf and Wise, 1994; Kristensen et al., 2001)
Assemblies			
Gold–silicon dioxide passivated microcircuit		Reactive	

Chronic implantation of any device into the central nervous system, even those materials considered biocompatible, elicits a common response consisting of encapsulation by macrophages, microglia, astrocytes, fibroblasts, endothelia and meningeal cells (Rudge et al., 1989). The early response to material implantation is inflammation (Stensaas and Stensaas, 1978; Rudge et al., 1989; Turner et al., 1999). The chronic response is characterized by a hypertrophy of the surrounding astrocytes (Stensaas and Stensaas, 1978) which display elevated expression of intermediate filament proteins such as GFAP and vimentin (Bignami and Dahl, 1976), an infiltration of microglia and foreign body giant cells (Stensaas and Stensaas, 1978) and a thickening of the surrounding tissue that forms a capsule around the device (Hoogerwerf and Wise, 1994; Turner et al., 1999).

The reversible charge storage capacity (CSC) of an electrode, also known as the reversible charge injection limit (Robblee and Rose, 1990), is the total amount of charge that may be stored reversibly, including storage in the double layer capacitance, pseudocapacitance, or any reversible Faradaic reaction. In electrical stimulation of excitable tissue it is desirable to have a large reversible charge stor-

age capacity so that a relatively large amount of charge may be injected (thus being efficacious for stimulation) prior to the onset of irreversible Faradaic reactions (which may be deleterious to the tissue being stimulated or to the electrode itself). The reversible charge storage capacity depends upon the material used for the electrode, the size and shape of the electrode, the electrolyte composition, and parameters of the electrical stimulation waveform.

The slow cyclic voltammogram for a material is a graphic display of the current density into various electrochemical processes as a function of the electrode potential as the potential is slowly cycled. At any point in time, the amount of current going into a particular process is determined by the potential as well as by the reactant concentration, as given by Eq. (1.17). The water window is defined as the potential region between the oxidation of water to form oxygen and the reduction of water to form hydrogen. Because water does not become mass transport limited in an aqueous solution, once the electrode potential attains either of these two water window boundaries, all further injected charge goes into the irreversible processes of water oxidation (anodically) or water reduction (cathodically). In many studies, the reversible charge storage capacity has been defined as the maximum charge density that can be applied without the electrode potential exceeding the water window during pulsing. It should be noted that in fact irreversible processes might occur at potentials within the water window, including such reactions as irreversible oxygen reduction (Merrill, in preparation) that may become mass transport limited.

The noble metals, including platinum (Pt), gold (Au), iridium (Ir), palladium (Pd), and rhodium (Rh), have been commonly used for electrical stimulation, largely due to their relative resistance to corrosion (Dymond et al., 1970; White and Gross, 1974; Johnson and Hench, 1977). These noble metals do exhibit some corrosion during electrical stimulation, as shown by dissolution (Brummer et al., 1977; Black and Hannaker, 1979; McHardy et al., 1980; Robblee et al., 1980, 1983a) and the presence of metal in the neighboring tissue (Robblee et al., 1983b; Tivol et al., 1987). In addition to corrosion of the electrode, there is evidence of long-term toxic effects on the tissue from dissolution (Rosenberg et al., 1965; Rosenberg, 1971; Macquet and Theophanides, 1976).

Platinum and platinum–iridium alloys are common materials used for electrical stimulation of excitable tissue. Brummer and Turner (1975, 1977a, 1977b, 1977c) have reported on the electrochemical processes of charge injection using a platinum electrode. They reported that three processes could store charge reversibly, including charging of the double layer capacitance, hydrogen atom plating and oxidation (pseudocapacity, reaction (1.6)) and reversible oxide formation and reduction on the electrode surface, and that 300–350 $\mu C/cm^2$ (real area) could theoretically be stored reversibly by these processes in artificial cerebrospinal fluid (equivalently 420–490 $\mu C/cm^2$ (geometric area)). This is a maximum reversible charge storage capacity under optimum conditions, including relatively long pulse widths (>0.6 ms). Rose and Robblee (1990) reported on the charge injection limits for a platinum electrode using 200 μs charge-balanced biphasic pulses. The reversible charge injection limit was defined as the maximum charge density that could be applied without the electrode potential exceeding the water window during pulsing. The authors determined the charge injection limit to be 50–100 $\mu C/cm^2$ (geometric) using anodic first pulses, and 100–150 $\mu C/cm^2$ (geometric) using cathodic first pulses. These values are considerably lower than the theoretical values determined by Brummer and Turner, since the electrode potential at the beginning of a pulse begins somewhere intermediate to oxygen and hydrogen evolution and not all of the three reversible processes accommodate charge during the stimulating pulse. Dissolution of platinum in saline increases linearly with the injected charge during biphasic stimulation (McHardy et al., 1980). Anodic first pulses cause more dissolution than cathodic first pulses, as the electrode potential attains more positive values during the stimulating (first) phase. Robblee et al. (1980) have shown that in the presence of protein such as serum albumin, the dissolution rate of platinum decreases by an order of magnitude.

The reversible charge storage capacity is dependent upon the electrode real surface area and geometry. The geometric area of an electrode is usually easily calculated, but the real area is the value that determines the total charge capacity. Brummer and Turner (1977b) have reported on a method to experimentally determine the real area of a platinum electrode in vitro, however, this may not be applicable to the in vivo situation. It should also be noted that the real area of an electrode may change during the course of stimulation. A non-uniform (non-spherical) electrode geometry will cause a non-uniform current density (Bruckenstein and Miller, 1970) with maximum current at the electrode edges, which may lead to localized electrode corrosion (Shepherd et al., 1985) or tissue burns (Wiley and Webster, 1982) at the electrode edges.

Platinum is a relatively soft material and may not be mechanically acceptable for all stimulation applications. Platinum is often alloyed with iridium to increase the mechanical strength. Alloys of platinum with 10–30% iridium have similar charge storage capacity to pure platinum (Robblee et al., 1983a). Iridium is a much harder metal than platinum, with mechanical properties that make it suitable as an intracortical electrode. The reversible charge storage capacities of bare iridium or rhodium are similar to that of platinum. However, when a surface oxide is present on either of these materials, they have greatly increased charge storage capacity over platinum. These electrodes inject charge using valency changes between two oxide states, without a complete reduction of the oxide layer.

Iridium oxide is a popular material for stimulation and recording, using reversible conversion between Ir^{3+} and Ir^{4+} states within an oxide to achieve high reversible charge storage capacity. Iridium oxide is commonly formed from iridium metal in aqueous electrolyte by electrochemical activation, which consists of repetitive potential cycling of iridium

to produce a multilayered oxide (Rand and Woods, 1974; Zerbino et al., 1978; Robblee et al., 1983a; Mozota and Conway, 1983; Robblee and Rose, 1990). Such activated iridium oxide films have been used for intracortical stimulation and recording using iridium wire (Bak et al., 1990; McCreery et al., 1992b; Loeb et al., 1995; Liu et al., 1999; Meyer and Cogan, 2001) or with micromachined silicon electrodes using sputtered iridium on the electrode sites (Anderson et al., 1989; Weiland and Anderson, 2000). The maximum charge density that can be applied without the electrode potential exceeding the water window was reported for activated iridium oxide using 200 μs charge-balanced pulses as ±2 mC/cm^2 (geometric) for anodic first pulsing and ±1 mC/cm^2 for cathodic first pulsing (Beebe and Rose, 1988; Kelliher and Rose, 1989). By using an anodic bias, cathodic charge densities of 3.5 mC/cm^2 (geometric) have been demonstrated both in vitro (Beebe and Rose, 1988; Kelliher and Rose, 1989) and in vivo (Agnew et al., 1986). Iridium oxide films can also be formed by thermal decomposition of an iridium salt onto a metal substrate (Robblee et al., 1986), or by reactive sputtering of iridium onto a metal substrate (Klein et al., 1989). Meyer and Cogan (2001) reported on a method to electrodeposit iridium oxide films onto substrates of gold, platinum, platinum–iridium and 316LVM stainless steel, achieving reversible charge storage capacities of >25 mC/cm^2.

The stainless steels (types 303, 316 and 316LVM) as well as the cobalt–nickel–chromium–molybdenum alloy MP35N are protected from corrosion by a thin passivation layer that develops when exposed to atmospheric oxygen and which forms a barrier to further reaction. In the case of stainless steel this layer consists of iron oxides, iron hydroxides and chromium oxides. These metals inject charge by reversible oxidation and reduction of the passivation layers. A possible problem with these metals is that if the electrode potential becomes too positive (the transpassive region), breakdown of the passivation layer and irreversible metal dissolution may occur at an unacceptable rate (Loucks et al., 1959; Greatbatch and Chardack, 1968; White and Gross, 1974), potentially leading to failure of the electrode. A cathodic charge imbalance has been shown to allow significantly increased charge injection without electrode corrosion (McHardy et al., 1977; Scheiner and Mortimer, 1990). Titanium and cobalt–chromium alloys are also protected from corrosion by a surface oxide passivation layer, and demonstrate better corrosion resistance than does stainless steel (reviewed by Gotman, 1997). 316LVM stainless steel has good mechanical properties and has been used for intramuscular electrodes. The charge storage capacity of 316LVM is only 40–50 μC/cm^2 (geometric), necessitating large surface area electrodes.

Capacitor electrodes inject charge strictly by capacitive action, as a dielectric material separates the metal electrode from the electrolyte, preventing Faradaic reactions at the interface (Guyton and Hambrecht, 1973, 1974; Rose et al., 1985). The tantalum/tantalum pentoxide (Ta/Ta_2O_5) electrode has a high charge storage capacity, achieved by using sintered tantalum or electrolytically etched tantalum wire to increase the surface area. Guyton and Hambrecht (1973, 1974) have demonstrated a sintered Ta/Ta_2O_5 electrode with a charge storage capacity of 700 μC/cm^2 (geometric). The Ta/Ta_2O_5 electrodes have sufficient charge storage capacity for electrodes in the range of 0.05 cm^2 and charge densities up to 200 μC/cm^2 (geometric); however, they may not be acceptable for microelectrode applications where the required charge densities may exceed 1 mC/cm^2 (Rose et al., 1985). Tantalum capacitor electrodes must operate at a relatively positive potential to prevent electron transfer across the oxide. If pulsed cathodically, a positive bias must be used on the electrode.

Stimulation of muscle, peripheral nerve or cortical surface requires relatively high charge per pulse (on the order of 0.2–5 μC), thus platinum or stainless steel electrodes must be of fairly large surface area to stay within the reversible charge storage capacity. Intracortical stimulation requires much less total charge per pulse, however, in order to achieve selective stimulation, the electrode size must be very small, resulting in high charge density requirements. With a geometric surface area of 20×10^{-6} cm^2, the charge per pulse may be on the order of 0.008–0.064 μC, yielding a charge density of 400–3200 μC/cm^2 (Agnew et al., 1986; McCreery et al., 1986). Such high charge densities may be achieved using iridium oxide electrodes with anodic pulses, or cathodic pulses with an anodic bias.

Table 2 lists several parameters of interest for materials commonly used for stimulation.

4. Principles of extracellular stimulation of excitable tissue

The goal of electrical stimulation of excitable tissue is often the triggering of action potentials in axons, which requires the artificial depolarization of some portion of the axon membrane to threshold. In the process of extracellular stimulation, the extracellular region is driven to relatively more negative potentials, equivalent to driving the intracellular compartment of a cell to relatively more positive potentials. Charge is transferred across the membrane due to both passive (capacitive and resistive) membrane properties as well as through active ion channels (Hille, 1984). The process of physiological action potential generation is well reviewed in the literature (e.g. *Principles of Neural Science* by Kandel et al., 2000), and models have been proposed (Chiu et al., 1979; Sweeney et al., 1987) for mammalian myelinated axons in terms of the parameters "*m*" and "*h*" as defined by Hodgkin and Huxley (1952a, 1952b, 1952c, 1952d) in their studies of the squid giant axon.

The mechanisms underlying electrical excitation of nerve have been reviewed elsewhere (McNeal, 1976; Ranck, 1981; Mortimer, 1990; Durand, 1995). In the simplest case of

Table 2
Reversible charge storage capacity and other parameters in electrode material selection

	Reversible charge storage capacity ($\mu C/cm^2$)	Reversible charge injection processes	Corrosion characteristics	Mechanical characteristics
Platinum	300–350 r[a]; AF, 200 μs: 50–100 g[b]; CF, 200 μs: 100–150 g[b]	Double layer charging, hydrogen atom plating, and oxide formation and reduction	Relatively resistant; greatly increased resistance with protein	Relatively soft
Platinum–iridium alloys	Similar CSC to Pt			Stronger than Pt
Iridium	Similar CSC to Pt			Stronger than Pt
Iridium oxide	AF: ±2200 g[c,d]; CF: ±1200 g[c,d]; AB: ±3500 g[c,d,e]	Oxide valency changes	Highly resistant[e,f]	
316LVM stainless steel	40–50 g	Passive film formation and reduction	Resistant in passive region; rapid breakdown in transpassive region	Strong and flexible
Tantalum/tantalum pentoxide	700 g[g]; 200 g[h]	Capacitive only	Corrosion resistant[i,j,k,l]	

r = real area; g = geometric area; AF = anodic first, charge-balanced; CF = cathodic first, charge-balanced; AB = cathodic first, charge-balanced, with anodic bias.

[a] Brummer and Turner (1977c).
[b] Rose and Robblee (1990).
[c] Beebe and Rose (1988).
[d] Kelliher and Rose (1989).
[e] Agnew et al. (1986).
[f] Robblee et al. (1983a).
[g] Guyton and Hambrecht (1973, 1974).
[h] Rose et al. (1985).
[i] Bernstein et al. (1977).
[j] Donaldson (1974).
[k] Johnson et al. (1977).
[l] Lagow et al. (1971).

stimulation, a monopolar electrode (a single current carrying conductor) is placed in the vicinity of excitable tissue. Current passes from the electrode, through the extracellular fluid surrounding the tissue of interest, and ultimately to a distant counter electrode. For a current I (in amps) flowing through the monopolar electrode located a distance r away from a segment of excitable tissue, and uniform conductivity in the fluid of σ (S/m), the extracellular potential V_e at the tissue is:

$$V_e = \frac{I}{4\pi\sigma r} \tag{4.1}$$

Bipolar and other electrode configurations have more complex voltage and current patterns and will not be discussed here. Durand (1995) has reviewed solutions for electrical potential profiles of various systems.

During current-controlled stimulation, the current is constant throughout the period of the pulse; thus, the V_e at any point in space is constant during the pulse. During V_{WE-CE} control, current is not constant throughout the period of the pulse (Fig. 6) and the V_e at any point decreases during the pulse.

The electric field generated by a monopolar electrode will interact with an axon membrane (these principles may be generalized to any excitable tissue). During cathodic stimulation, the negative charge of the working electrode causes a redistribution of charge on the axon membrane, with negative charge collecting on the outside of the membrane underneath the cathode (depolarizing the membrane). Associated with the depolarization of the membrane under the cathode is movement of positive charge intracellularly from the distant axon to the region under the electrode, and hyperpolarization of the membrane at a distance away from the electrode. If the electrode is instead driven as an anode (to more positive potentials), hyperpolarization occurs under the anode, and depolarization occurs at a distance away from the anode. Action potentials may be initiated at the regions distant from the electrode where depolarization occurs, known as virtual cathodes. The depolarization that occurs with such anodic stimulation is roughly one-seventh to one-third that of the depolarization with cathodic stimulation; thus, cathodic stimulation requires less current to bring an axon to threshold. During cathodic stimulation, anodic surround block may occur at sufficiently high current levels, where the hyperpolarized regions of the axon distant from the cathode may suppress an action potential that has been initiated near the electrode. This effect is observed at higher current levels than the threshold values required for initiation of action potentials with cathodic stimulation.

In a mammalian axon, hyperpolarizing with a pulse that is long compared with the time constant of the sodium inactivation gate will remove the normal partial inactivation. If the hyperpolarizing current is then abruptly terminated (as with a rectangular pulse), the sodium activation gate conductance increases back to the rest value relatively quickly, but the activity of the slower inactivation gate remains high for a

period of milliseconds; thus, the net sodium conductance is briefly higher than normal and an action potential may be initiated. This phenomenon, known as anodic break, may be observed with either cathodic or anodic stimulation, since both cause some region of hyperpolarization in the axon. Anodic break may be prevented by using stimulating waveforms with slowly decaying exponential phases instead of abrupt terminations (van den Honert and Mortimer, 1979, 1981a, 1981b; Fang and Mortimer, 1991a).

Prolonged subthreshold stimuli can produce the phenomenon of accommodation. A cathodic pulse to mammalian axon that produces subthreshold depolarization will increase sodium inactivation, reducing the number of axons that can be recruited and so increasing the threshold. This is not a problem with brief pulses that are shorter than the time constant of sodium channel inactivation, but can be with more prolonged pulses.

It is often desirable to have some degree of selectivity during electrical excitation of tissue. Selectivity is the ability to activate one population of neurons without activating a neighboring population. Spatial selectivity is the ability to activate a localized group of neurons, such as restricting activation to a certain fascicle or fascicles within a nerve trunk. Changes in the transmembrane potential due to electrical excitation are greatest in fibers closest to the stimulating electrode because the induced extracellular potential decreases in amplitude with distance from the stimulation electrode (Eq. (4.1)), as does the second spatial derivative of the extracellular potential, which is responsible for excitation (Rall, 1977). Thus, activation of neurons closest to the electrode requires the least current. As the distance between the electrode and desired population of neurons for activation increases, larger currents are required, which generally means neurons between the electrode and desired population are also activated. Fiber diameter selectivity is the ability to activate fibers within a certain range of diameters only. Fibers with greater internodal distance and larger diameter experience greater changes in the transmembrane potential due to electrical excitation (Rattay, 1989). Using conventional electrical stimulation waveforms with relatively narrow pulses, the largest diameter fibers are activated at the lowest stimulus amplitude. In motor nerves, activating large diameter fibers first corresponds to activating the largest motor units first. This recruitment order is opposite of the physiological case where the smallest motor units are recruited first. Fang and Mortimer (1991a) have demonstrated a waveform that allows a propagated action potential in small diameter fibers but not large diameter fibers. Hyperpolarizing pulses have a greater effect on larger fibers than smaller, just as for depolarizing pulses. This means that sustained hyperpolarization can be used to block action potential initiation selectively in the large fibers, so that the corresponding depolarizing stimuli can selectively activate small fibers. Electrical stimulation protocols have also been developed (McIntyre and Grill, 2002) for triggering of action potentials in specific cell types (e.g. interneurons) and structures (e.g. nerve terminals).

The relationship between the strength (current) of an applied constant current pulse required to initiate an action potential and the duration of the pulse, known as the strength–duration curve, is shown in Fig. 7(a). The threshold current I_{th} decreases with increasing pulse width. At very long pulse widths, the current is a minimum, called the rheobase current I_{rh}. The following relationship has been derived experimentally to quantify the strength–duration curve (Lapicque, 1907):

$$I_{th} = \frac{I_{rh}}{1 - \exp(-W/\tau_m)} \tag{4.2}$$

where I_{th} is the current required to reach threshold, I_{rh} is the rheobase current, W is the pulse width, and τ_m is the membrane time constant. The qualitative nature of the strength–duration curve shown is representative of typical excitable tissue. The quantitative aspects, e.g. the rheobase current, depend upon factors such as the distance between the neuron population of interest and the electrode, and are determined empirically. Fig. 7(b) illustrates the charge–duration curve, which plots the threshold charge $Q_{th} = I_{th}W$ versus pulse width. At longer pulse widths, the required charge to elicit an action potential increases, due to two phenomena. First, over a period of tens to hundreds of μs, charge is redistributed through the length of the axon, and does not all participate in changing the transmembrane potential at the site of injection (Warman et al., 1992; Plonsey and Barr, 1988). Second, over a period of several ms, accommodation (increased sodium inactivation) occurs. The minimum charge Q_{min} occurs as the pulse width approaches zero. In practice, the Q_{th} is near Q_{min} when narrow pulses are used (tens of microseconds).

It is generally best to keep the pulse width narrow in order to minimize any electrochemical reactions occurring on the electrode surface. The narrowness of a pulse is often limited by the amount of current that can be delivered by a stimulator, especially if it is battery operated. Furthermore, some kinds of stimulation, such as selective activation of certain axons of a nerve, require pulses longer than tens of microseconds.

5. Mechanisms of damage

An improperly designed electrical stimulation system may cause damage to the tissue or damage to the electrode itself. Damage to an electrode can occur in the form of corrosion if the electrode is driven anodically such that the electrode potential exceeds a value where significant metal oxidation occurs. An example of such a reaction is the corrosion of platinum in a chloride-containing medium such as extracellular fluid (Eq. (1.10)). Corrosion is an irreversible Faradaic process. It may be due to dissolution where the electrochemical product goes into solution, or the product may form an outer solid layer on a passivation film that cannot be recovered. Charge-balanced waveforms (Fig. 3(b)) are more likely to reach potentials where corrosion may occur during the anodic

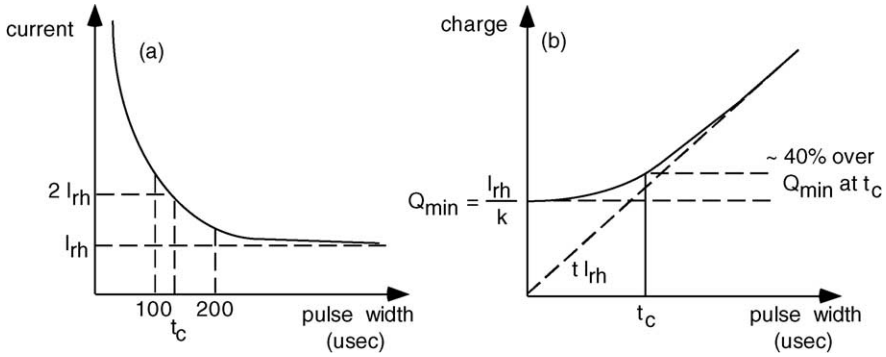

Fig. 7. Strength–duration and charge–duration curves for initiation of an action potential. Rheobase current I_{rh} is the current required when using an infinitely long pulse width. Chronaxie time t_c is the pulse width corresponding to two times the rheobase current.

reversal phase and the open circuit interpulse interval than are monophasic waveforms (Fig. 4). The charge-imbalanced waveform (Fig. 3(c)) has advantages both in preventing tissue damage due to sustained negative potentials during the interpulse interval, and in preventing corrosion by reducing the maximum positive potential during the anodic reversal phase (Section 2).

The mechanisms for stimulation induced tissue damage are not well understood. Two major classes of mechanisms have been proposed. The first is that tissue damage is caused by intrinsic biological processes as excitable tissue is overstimulated. This is called the mass action theory, and proposes that damage occurs from the induced hyperactivity of many neurons firing, or neurons firing for an extended period of time, thus changing the local environment. Proposed mass action mechanisms include depletion of oxygen or glucose, or changes in ionic concentrations both intracellularly and extracellularly, e.g. an increase in extracellular potassium. In the CNS, excessive release of excitatory neurotransmitters such as glutamate may cause excitotoxicity. The second proposed mechanism for tissue damage is the creation of toxic electrochemical reaction products at the electrode surface during cathodic stimulation at a rate greater than that which can be tolerated by the physiological system.

McCreery et al. (1988) have shown that when identical charge-balanced stimulation protocols were applied to platinum stimulating electrodes (known to participate in Faradaic reactions) and tantalum pentoxide stimulating electrodes (considered to be strictly capacitive (reversible) in action), the tissue damage induced in cat brain during stimulation was not statistically different. The authors concluded that the damage induced in the cortex under the conditions of stimulation used was due to passage of current through the tissue, not due to electrochemical reaction products. Agnew et al. (1990) studied stimulation of cat peroneal nerve, and concluded that the damage to an axon is due to the total induced neural activity having some effect on the extraaxonal environment. Agnew et al. (1993) came to similar conclusions in studies of electrical stimulation of the cat brain. The authors concluded that neural injury from prolonged electrical stimulation is linked to neuronal activity produced by the stimulation, and furthermore that injury derives at least in part from entry of calcium into the neurons, consistent with the mass action hypothesis. The authors state that:

"The most useful hypothesis may be that the activation of excitatory amino acid receptors does not 'cause' neural injury, but merely lowers its threshold in response to a given stressor by magnifying the destructive effect of the stressor, and that the manner and degree to which this occurs depends upon the physical and pharmacological composition of the particular neural substrate, as well as the stimulus parameters."

Such an interpretation indicates how the mass action and electrochemical theories of tissue damage are not exclusive.

McCreery et al. (1990) have shown that both charge per phase and charge density are important factors in determining neuronal damage to cat cerebral cortex. In terms of the mass action theory of damage, charge per phase determines the total volume within which neurons are excited, and the charge density determines the proportion of neurons close to an electrode that are excited; thus, both factors determine the total change in the extracellular environment. The McCreery data show that as the charge per phase increases the charge density for safe stimulation decreases. When the total charge is small (as with a microelectrode) a relatively large charge density may safely be used. Tissue damage that has been attributed to mass action effects may be alternatively explained by electrochemical means, as charge and charge density may influence the quantity of irreversible reaction products being generated at the electrode interface. Shannon (1992) reprocessed the McCreery data and developed an expression for the maximum safe level for stimulation, given by:

$$\log\left(\frac{Q}{A}\right) = k - \log(Q) \tag{5.1}$$

where Q is charge per phase (μC per phase), Q/A is charge density per phase (μC/cm^2 per phase), and $2.0 > k > 1.5$, fit to the empirical data.

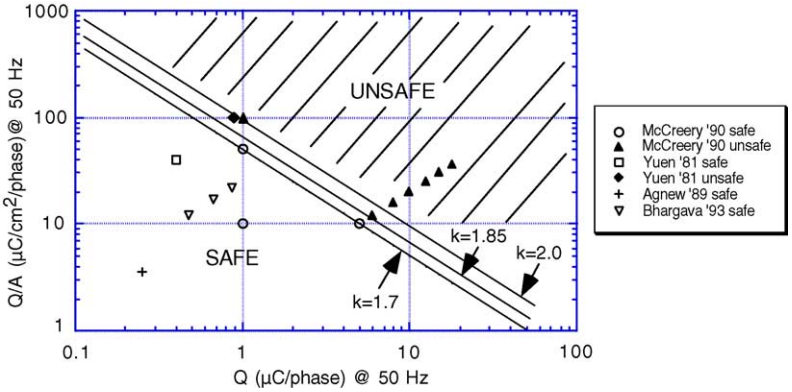

Fig. 8. Charge (Q) vs. charge density (Q/A) for safe stimulation. A microelectrode with relatively small total charge per pulse might safely stimulate using a large charge density, whereas a large surface area electrode (with greater total charge per pulse) must use a lower charge density.

Fig. 8 illustrates the charge vs. charge density relationship of Eq. (5.1) using k values of 1.7, 1.85 and 2.0, with histological data from the 1990 McCreery study using cat parietal cortex as well as data from Yuen et al. (1981) on cat parietal cortex, Agnew et al. (1989) on cat peroneal nerve, and Bhargava (1993) on cat sacral anterior roots. Above the threshold for damage, experimental data demonstrates tissue damage, and below the threshold line, experimental data indicate no damage.

McCreery et al. (1992a) have reviewed damage from electrical stimulation of peripheral nerve. They concluded that damage may be from mechanical constriction of the nerve as well as neuronal hyperactivity and irreversible reactions at the electrode.

Supporting the concept that damage is due to electrochemical reaction products is the work by Lilly et al. (1952), which demonstrated that loss of electrical excitability and tissue damage occurs when the cerebral cortex of monkey is stimulated using monophasic current pulses. Later, Lilly et al. (1955) showed that biphasic stimulation caused no loss of excitability or tissue damage after 15 weeks of stimulation for 4–5 h per day. Lilly interpreted these results as due to movement of charged particles such as proteins out of physiological position. The concept that monophasic is a more damaging form of stimulation than charge-balanced biphasic was confirmed by Mortimer et al. (1970), who reported that breakdown of the blood–brain barrier during stimulation of the surface of cat cerebral cortex occurs when monophasic pulses were used at power densities greater than 0.003 W/in.^{2} (0.5 mW/cm^2), but does not occur with charge-balanced biphasic pulses until a power density of 0.05 W/in.^{2} (8 mW/cm^2) is exceeded. Pudenz et al. (1975a, 1975b) further showed that monophasic stimulation of the cat cerebral cortex causes vasoconstriction, thrombosis in venules and arterioles and blood–brain barrier breakdown within 30 s of stimulation when used at levels required for a sensorimotor response; however, charge-balanced biphasic stimulation could be used for up to 36 h continuously without tissue damage if the charge per phase was below 0.45 μC (4.5 μC/cm^2). Also supporting the hypothesis that damage is due to electrochemical products are observations of cat muscle that suggest some non-zero level of reaction product can be tolerated (Mortimer et al., 1980; Scheiner and Mortimer, 1990). These studies showed that monophasic stimulation causes significantly greater tissue damage than a non-stimulated implant at 1 μC/mm^2 per pulse but not 0.2 μC/mm^2 per pulse, and that charge-balanced biphasic stimulation does not cause significant tissue damage at levels up to 2 μC/mm^2 per pulse. However, in order to prevent electrode corrosion, the charge-balanced waveform must not exceed 0.4 μC/mm^2 per pulse, otherwise the electrode potential is driven to damaging positive potentials during the anodic (reversal) phase and interpulse interval. Scheiner and Mortimer (1990) studied the utility of charge-imbalanced biphasic stimulation, demonstrating that this waveform allows greater cathodic charge densities than monophasic prior to the onset of tissue damage as reactions occurring during the cathodic phase are reversed by the anodic phase, and also that greater cathodic charge densities can be used than with the charge-balanced waveform prior to electrode corrosion since the anodic phase is no longer constrained to be equal to the cathodic phase, thus the electrode potential reaches less positive values during the anodic phase and interpulse interval. Scheiner found that cat muscle tissue was significantly damaged using monophasic stimulation at 0.4 μC/mm^2 per phase, and that when charge-imbalanced biphasic stimulation was used, tissue was damaged with 1.2 μC/mm^2 per phase cathodic and 0.2 μC/mm^2 per phase anodic, and could safely tolerate 1.2 μC/mm^2 per phase cathodic and 0.5 μC/mm^2 per phase anodic. No electrode corrosion was observed under any of the conditions studied.

In 1975, Brummer and Turner gave an alternative explanation to Lilly's for why biphasic pulses were less damaging than monophasic. They proposed that two principles should be followed to achieve electrochemically safe conditions during tissue stimulation:

"(1) Perfect symmetry of the electrochemical processes in the two half-waves of the pulses should be sought. This implies

that we do not generate any electrolysis products in solution. One approach to achieve this would appear to involve the use of perfectly charge-balanced waveforms of controlled magnitude. (2) The aim should be to inject charge via non-Faradaic or surface-Faradaic processes, to avoid injecting any possibly toxic materials into the body."

Their model for safe stimulation interprets the charge-balanced waveform in electrochemical terms. Any process occurring during the first (stimulating) phase, whether it is charging of the electrode or a reversible Faradaic process, is reversed during the second (reversal) phase, with no net charge delivered. The observation that monophasic stimulation causes greater tissue damage than biphasic stimulation at the same amplitude, pulse width and frequency is explained by the fact that during monophasic stimulation, all injected charge results in generation of electrochemical reaction products.

Reversible processes include charging and discharging of the double layer capacitance, as well as surface bound reversible Faradaic processes such as reactions (1.3)–(1.8) and (1.13). Reversible reactions often involve the production or consumption of hydrogen or hydroxyl ions as the charge counterion. This causes a change in the pH of the solution immediately adjacent to the electrode surface. Ballestrasse et al. (1985) gave a mathematical description of these pH changes, and determined that the pH may range from 4 to 10 near a 1 μm diameter electrode during biphasic current pulses, but this change extended for only a few μm. Irreversible processes include Faradaic reactions where the product does not remain near the electrode surface, such as reactions (1.1) and (1.9)–(1.12).

Free radicals are known to cause damage to myelin, the lipid cell membrane and DNA of cells. A likely candidate for a mechanism of neural tissue damage due to electrochemical products is peroxidation of the myelin by free radicals produced on the electrode surface. Several researchers (Chan et al., 1982; Chia et al., 1983; Konat and Wiggins, 1985; Sevanian, 1988; Griot et al., 1990; Buettner, 1993) have demonstrated the great susceptibility of myelin to free radical damage. Damage occurs as fatty acyl chains move apart and the myelin goes from a crystalline (ordered) state to a liquid (disordered) state.

Morton et al. (1994) have shown that oxygen reduction occurs on a gold electrode in phosphate buffered saline under typical neural stimulating conditions. Oxygen reduction reactions that may occur during the cathodic stimulating phase include reactions that generate free radicals such as superoxide and hydroxyl, and hydrogen peroxide, collectively known as reactive oxygen species. These species may have multiple deleterious effects on tissue (reviewed by Halliwell, 1992; Stohs, 1995; Hemnani and Parihar, 1998; Imlay, 2003; Bergamini et al., 2004). As free radicals are produced they may interfere with chemical signaling pathways that maintain proper perfusion of nervous tissue. Nitric oxide has been identified as the endothelium derived relaxing factor, the primary vasodilator (Furchgott, 1988; Ignarro et al., 1988; Umans and Levi, 1995). Nitric oxide is also known to prevent platelet aggregation and adhesion (Azuma et al., 1986; Radomski et al., 1987; Moncada et al., 1991). Beckman et al. (1990) have shown that the superoxide radical reacts with nitric oxide to form the peroxynitrite radical. Oxygen-derived free radicals from the electrode may reduce the nitric oxide concentration and diminish its ability as the principal vasodilator and as an inhibitor of platelet aggregation. Superoxide depresses vascular smooth muscle relaxation by inactivating nitric oxide, as reviewed by Rubanyi (1988).

An electrochemical product may accumulate to detrimental concentrations if the rate of Faradaic reaction, given by the current–overpotential relationship of Eq. (1.17), exceeds the rate for which the physiological system can tolerate the product. For most reaction products of interest there is some sufficiently low concentration near the electrode that can be tolerated over the long term. This level for a tolerable reaction may be determined by the capacity of an intrinsic buffering system. For example, changes in pH are buffered by several systems including the bicarbonate buffer system, the phosphate buffer system, and intracellular proteins. The superoxide radical, a product of the reduction of oxygen, is converted by superoxide dismutase and cytochrome *c* to hydrogen peroxide and oxygen. The diffusion rate of a toxic product must be considered, as it may be the case that high concentrations only exist very near the site of generation (the electrode surface).

6. Design of efficacious and safe electrical stimulation

A stimulating system must be both efficacious and safe. Efficacy of stimulation generally means the ability to elicit the desired physiological response, which can include initiation or suppression of action potentials. Safety has two primary aspects. First, the tissue being stimulated must not be damaged, and second, the stimulating electrode itself must not be damaged, as in corrosion. An electrode implanted into a human as a prosthesis may need to meet these requirements for decades. In animal experimentation, damage to the tissue or the electrode can seriously complicate or invalidate the interpretation of results.

Efficacy requires that the charge injected must exceed some threshold (Fig. 7), however, as the charge per pulse increases, the overpotential of the electrode increases as does the fraction of the current going into Faradaic reactions (which may be damaging to tissue or the electrode). Judicious design of stimulation protocols involves acceptable compromises between stimulation efficacy, requiring a sufficiently high charge per pulse, and safety, requiring a sufficiently low charge per pulse, thus preventing the electrode from reaching potentials where deleterious Faradaic reactions occur at an intolerable rate. The overpotential an electrode reaches, and thus Faradaic reactions that can occur, depend on several factors in addition to the charge per pulse, including:

(1) waveform type (Fig. 4); (2) stimulation frequency; (3) electrode material (a high charge storage capacity allows relatively large charge storage prior to reaching overpotentials where irreversible Faradaic reactions occur); (4) electrode geometric area and roughness (determining real area) and therefore total capacitance; and (5) train effects (Section 2). Increasing either the stimulus phase pulse width or the reversal phase pulse width of a charge-balanced stimulation protocol has the effect of increasing unrecoverable charge into irreversible reactions. Any factor which either drives the electrode potential into a range where irreversible reactions occur (such as a long stimulus phase pulse width) or fails to quickly reverse the electrode potential out of this range (such as a long reversal phase pulse width) will allow accumulation of unrecoverable charge.

The overpotential an electrode must be driven to before any given current will be achieved is highly dependent on the kinetics of the system, characterized by the exchange current density i_0. For a system with a large exchange current density (e.g. $i_0 = 10^{-3}$ A/cm^2), no significant overpotential may be achieved before a large Faradaic current ensues (Eq. (1.17)). When i_0 is many orders of magnitude smaller (e.g. $i_0 = 10^{-9}$ A/cm^2), a large overpotential must be applied before there is substantial Faradaic current. When i_0 is very low, a large total charge can be injected through the capacitive mechanism before significant Faradaic reactions commence. This is the generally desirable paradigm for a stimulating electrode, minimizing Faradaic reactions that lead to either electrode damage or tissue damage.

The fundamental design criteria for a safe stimulation protocol can be stated: *the electrode potential must be kept within a potential window where irreversible Faradaic reactions do not occur at levels that are intolerable to the physiological system or the electrode*. If irreversible Faradaic reactions do occur, one must ensure that they can be tolerated (e.g. that physiological buffering systems can accommodate any toxic products) or that their detrimental effects are low in magnitude (e.g. that corrosion occurs at a very slow rate, and the electrode will last for longer than its design lifetime).

The charge–duration curve shown in Fig. 7 demonstrates that to minimize the total charge injected in an efficacious stimulation protocol, one should use short duration pulses. In practice, pulses on the order of tens of microseconds approach the minimum charge, and are often reasonable design solutions. During this relatively short duration one may be able to avoid Faradaic reactions that would occur at higher levels of total charge with longer pulses. While it is desirable to use short duration pulses on the order of tens of microseconds, there are applications for which biological constraints require longer duration pulses. The time constants of several key ion channels in the membranes of excitable tissue are measured in hundreds of microseconds to milliseconds. By using stimulating pulses with comparable durations one can selectively manipulate the opening and closing of these ion channels to accomplish various specific behaviors. Certain waveforms have been developed that allow selectivity during electrical excitation of tissue (Section 4). Grill and Mortimer (1995) have reviewed stimulus waveforms used for spatial and fiber diameter selective neural stimulation, illustrating the response of the neural membrane to different waveforms. Selective waveforms often require stimulation or reversal phases with long pulse widths relative to conventional stimulus waveforms; thus, waveforms optimized for physiological responses may not be efficient for reversing electrochemical processes. Judicious design of electrical protocols has allowed the designers of neural prostheses to selectively inactivate the larger neurons in a nerve trunk (Fang and Mortimer, 1991b), selectively inactivate the superficial fibers in a nerve by pre-conditioning (Grill and Mortimer, 1997), and prevent anodic break. Lastly, there are applications where tonic polarization mandates the use of very long (>1 s) monophasic pulses; for example, tonic hyperpolarization of the soma to control epileptic activity (Gluckman et al., 1996; Ghai et al., 2000). The use of these various waveforms with long pulse widths allows greater accumulation of any electrochemical product, thus requiring additional diligence by a neurophysiologist or prosthesis designer to prevent electrochemical damage.

In addition to biological constraints on the pulse durations, the required current for a short pulse width may also be a limitation. In order to inject the minimum charge required for effect, a large current is required (Fig. 7). This is not always possible, as may be the case with a battery powered stimulator with limited current output.

Certain applications, such as clinical deep brain stimulation (McIntyre and Thakor, 2002; O'Suilleabhain et al., 2003) and experimental long-term potentiation (Bliss and Lomo, 1973) require the use of high frequency (>50 Hz) pulsing. As discussed in Section 2, this can lead to a ratcheting of the electrode potential not achieved during single pulse stimulation. Appropriate design of stimulation protocols can minimize damage by careful attention to the effects of high frequency stimulation on the electrode potential.

Fig. 9 summarizes key features of various stimulation waveform types. The cathodic monophasic waveform illustrated in Fig. 9(a) consists of pulses of current passed in one direction, with an open circuit condition during the interpulse interval. At no time does current pass in the opposite direction. Commonly the working electrode is pulsed cathodically for stimulation of tissue (as shown), although anodic stimulation may also be used (Section 4). Of the waveforms illustrated in Fig. 9, the monophasic is the most efficacious for stimulation. However, monophasic pulses are not used in long-term stimulation where tissue damage is to be avoided. Greater negative overpotentials are reached during monophasic pulsing than with biphasic pulsing (Fig. 4). Furthermore, the electrode potential during the interpulse interval of cathodic monophasic pulsing remains relatively negative as the charged electrode capacitance slowly discharges through Faradaic reactions, allowing reduction reactions which may be deleterious to tissue to proceed throughout the entire period of stimulation. Biphasic waveforms are illustrated in

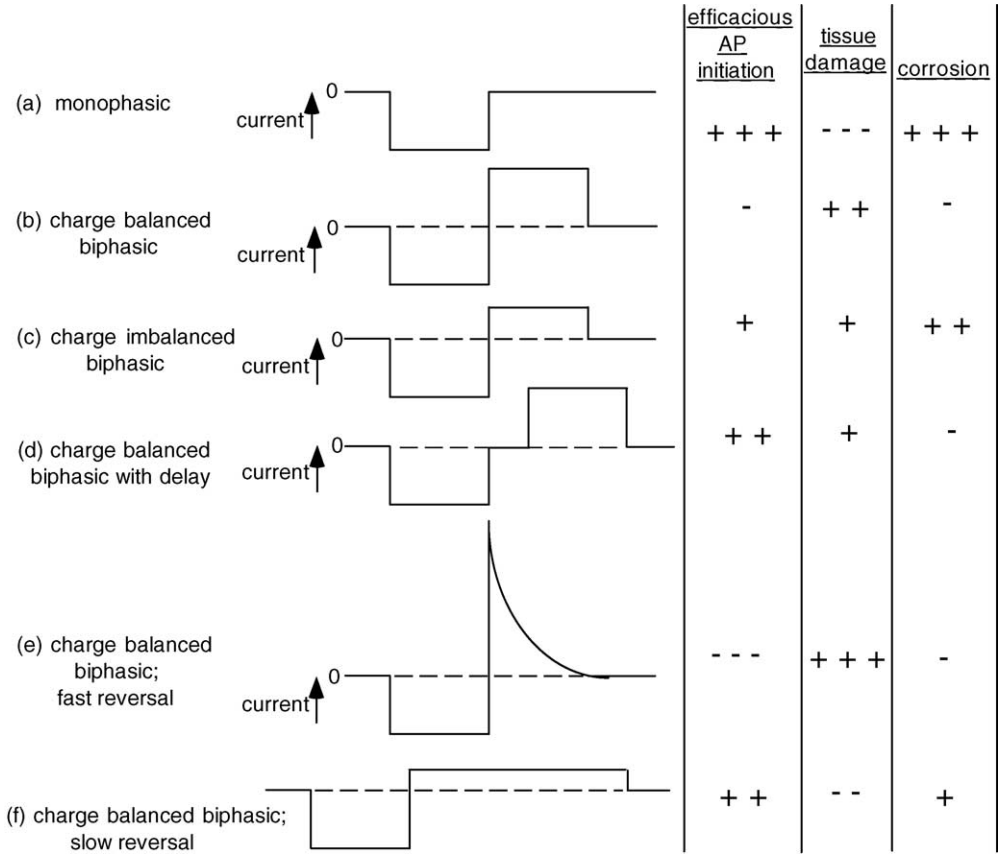

Fig. 9. Comparison of stimulating waveforms. Six prototypical waveforms are rated for relative merit in efficacy and safety: "+++" = best (most efficacious, least damaging to tissue or the electrode); "−−−" = worst.

Fig. 9(b)–(f). The first (stimulating) phase elicits the desired physiological effect such as initiation of an action potential, and the second (reversal) phase is used to reverse the direction of electrochemical processes occurring during the stimulating phase (Section 2). If all processes of charge injection during the stimulating phase are reversible, then the reversal phase will prevent net changes in the chemical environment of the electrode, as desired. The charge-balanced biphasic waveform (Fig. 9(b)) is widely used to prevent tissue damage. It should be noted that charge balance does not necessarily equate to electrochemical balance. As given by Eqs. (2.6) and (2.7), during certain instances of stimulation, there are irreversible Faradaic reactions during the cathodic phase (e.g. oxygen reduction), and then different irreversible reactions during the anodic phase (e.g. electrode corrosion) that are not the reverse of the cathodic Faradaic reactions. Such electrochemical imbalance leads to a potential waveform as illustrated in Fig. 4(b), where the potential at the end of the anodic phase is positive of the pre-pulse potential, allowing irreversible reactions such as electrode corrosion to occur. The charge-imbalanced waveform, illustrated in Fig. 9(c), may be used to reduce the most positive potentials during the anodic phase with respect to the charge-balanced waveform, and prevent electrode corrosion (Scheiner and Mortimer, 1990). Ideally, the charge in the reversal phase is equal to the charge going into reversible processes during the stimulation phase, in which case the electrode potential returns to its pre-pulse value at the end of the reversal phase.

In addition to electrode corrosion, a second concern with the charge-balanced biphasic waveform is that the reversal phase not only reverses electrochemical processes of the stimulation phase, but may also reverse some of the desired physiological effect of the stimulation phase, i.e. it may suppress an action potential that would otherwise be induced by a monophasic waveform. This effect causes an increased threshold for biphasic stimulation relative to monophasic. Gorman and Mortimer (1983) have shown that by introducing an open circuit interphase delay between the stimulating and reversal phases, the threshold for biphasic stimulation is similar to that for monophasic. This is illustrated in Fig. 9(d). Although the introduction of an interphase delay improves threshold, it also allows the electrode potential to remain relatively negative during the delay period. A delay of 100 μs is typically sufficient to prevent the suppressing effect of the reversal phase, and may be a short enough period that deleterious Faradaic reaction products do not accumulate to an unacceptable level.

As illustrated in Fig. 9(e) and (f), the more rapidly charge is injected during the anodic reversal phase, the more quickly the electrode potential is brought out of the most negative

range, and thus the less likely that tissue damage will occur. A high current reversal phase, however, means more of a suppressing effect on action potential initiation, and also means the electrode potential will move positive during the reversal phase, thus risking electrode corrosion.

When evaluating the electrochemistry of a stimulating electrode system, both the working electrode and counter electrode should be considered. If the area, and thus total capacitance, of a counter electrode is relatively large, there is a small potential change for a given amount of injected charge. Such an electrode will not be perturbed away from its resting potential as readily as a small electrode, and all charge injection across this large counter electrode is assumed to be by capacitive charging, not Faradaic processes. If the working electrode is driven cathodically first in a biphasic waveform (and thus the counter electrode anodically), then during the reversal phase the working electrode is driven anodically and the counter electrode cathodically. In such a system the working electrode is often referred to simply as the cathode. Strictly speaking, the working electrode is the cathode during the stimulus phase, and during the reversal phase the roles are reversed so that the working electrode is the anode and the counter electrode is the cathode.

This review has presented several issues to be considered in the selection of an electrode material and protocol for stimulation that are both efficacious and safe to the tissue and the electrode. Six requirements for the choice of a material were discussed (Section 3). Efficacy was presented in terms of injecting a sufficient charge, while the sometimes conflicting objective of safety was stated as requiring that the injected charge, and thus the overpotential an electrode reaches and Faradaic reaction product produced, is kept to a minimum. Section 6 summarized the relative merits of some common stimulating waveforms in achieving efficacy and safety.

Acknowledgements

The authors gratefully acknowledge financial support from NIH-NINDS under Ruth L. Kirschstein NRSA Fellowship 5F32NS045454, and Wellcome Trust, Department of Health and Medical Research Council.

References

Agnew WF, Yuen TGH, McCreery DB, Bullara LA. Histopathologic evaluation of prolonged intracortical electrical stimulation. Exp Neurol 1986;92:162–85.

Agnew WF, McCreery DB, Yuen TGH, Bullara LA. Histologic and physiologic evaluation of electrically stimulated peripheral nerve: considerations for the selection of parameters. Ann Biomed Eng 1989;17:39–60.

Agnew WF, McCreery DB, Yuen TGH, Bullara LA. Local anesthetic protects against electrically-induced neural damage in peripheral nerve. J Biomed Eng 1990;12:301–8.

Agnew WF, McCreery DB, Yuen TGH, Bullara LA. MK-801 protects against neuronal injury induced by electrical stimulation. Neuroscience 1993;52(1):45–53.

Anderson DJ, Najafi K, Tanghe SJ, Evans DA, Levy KL, Hetke JF, et al. Batch-fabricated thin-film electrodes for stimulation of the central auditory system. IEEE Trans Biomed Eng 1989;36:693–704.

Azuma H, Ishikawa M, Sekizaki S. Endothelium-dependent inhibition of platelet aggregation. Br J Pharmacol 1986;88:411–5.

Babb TL, Kupfer W. Phagocytic and metabolic reactions to chronically implanted metal brain electrodes. Exp Neurol 1984;86(2):171–82.

Bak MK, Girvin JP, Hambrecht FT, Kufta CV, Loeb GE, Schmidt EM. Visual sensations produced by intracortical microstimulation of the human occipital cortex. Med Biol Eng Comput 1990;28:257–9.

Ballestrasse CL, Ruggeri RT, Beck TR. Calculations of the pH changes produced in body tissue by a spherical stimulation electrode. Ann Biomed Eng 1985;13:405–24.

Bard AJ, Faulkner LR. Electrochemical methods. New York: Wiley; 1980 p. 19 and 102 [Chapters 1.3.3, 2, 3.5 and 9.1.3].

Beckman JS, Beckman TW, Chen J, Marshall PA, Freeman BA. Apparent hydroxyl radical production by peroxynitrite: implications for endothelial injury from nitric oxide and superoxide. Proc Natl Acad Sci USA 1990;87:1620–4.

Beebe X, Rose TL. Charge injection limits of activated iridium oxide electrodes with 0.2 ms pulses in bicarbonate buffered saline. IEEE Trans Biomed Eng 1988;BME-35:494–5.

Bergamini CM, Gambetti S, Dondi A, Cervellati C. Oxygen, reactive oxygen species and tissue damage. Curr Pharm Des 2004;10(14):1611–26.

Bernstein JJ, Hench LL, Johnson PF, Dawson WW, Hunter G. Electrical stimulation of the cortex with Ta_2O_5 capacitive electrodes. In: Hambrecht FT, Reswick JB, editors. Functional electrical stimulation. New York: Marcel Dekker; 1977. p. 465–77.

Bhargava A. Long-term effects of quasi-trapezoidal pulses on the structure and function of sacral anterior roots. M.S. thesis, Department of Biomedical Engineering, Case Western Reserve University, Cleveland, OH, 1993.

Bignami A, Dahl D. The astroglial response to stabbing: immunofluorescence studies with antibodies to astrocyte-specific protein (GFA) in mammalian and sub-mammalian vertebrate. Neuropathol Appl Neurobiol 1976;251:23–43.

Black RD, Hannaker P. Dissolution of smooth platinum electrodes in biological fluids. Appl Neurophysiol 1979;42:366–74.

Bliss TV, Lomo T. Long-lasting potentiation of synaptic transmission in the dentate area of the anaesthetized rabbit following stimulation of the perforant path. J Physiol 1973;232(2):331–56.

Bogdanski D, Koller M, Muller D, Muhr G, Bram M, Buchkremer HP, et al. Easy assessment of the biocompatibility of Ni–Ti alloys by in vitro cell culture experiments on a functionally graded Ni–NiTi–Ti material. Biomaterials 2002;22(23):4549–55.

Bruckenstein S, Miller B. An experimental study of non-uniform current distribution at rotating disk electrodes. J Electrochem Soc 1970;117:1044–8.

Brummer SB, Turner MJ. Electrical stimulation of the nervous system: the principle of safe charge injection with noble metal electrodes. Bioelectrochem Bioenerg 1975;2:13–25.

Brummer SB, Turner MJ. Electrochemical considerations for safe electrical stimulation of the nervous system with platinum electrodes. IEEE Trans Biomed Eng 1977a;BME-24:59–63.

Brummer SB, Turner MJ. Electrical stimulation with Pt electrodes. I. A method for determination of 'real' electrode areas. IEEE Trans Biomed Eng 1977b;BME-24:436–9.

Brummer SB, Turner MJ. Electrical stimulation with Pt electrodes. II. Estimation of maximum surface redox (theoretical non-gassing) limits. IEEE Trans Biomed Eng 1977c;BME-24:440–3.

Brummer SB, McHardy J, Turner MJ. Electrical stimulation with Pt electrodes: trace analysis for dissolved platinum and other dissolved electrochemical products. Brain Behav Evol 1977;14:10–22.

Buettner GR. The pecking order of free radicals and antioxidants: lipid peroxidation, alpha-tocopherol, and ascorbate. Arch Biochem Biophys 1993;300(2):535–43.

Chan PH, Yurko M, Fishman R. Phospholipid degradation and cellular edema induced by free radicals in brain slice cortical slices. J Neurochem 1982;38:525–31.

Chapman DL. A contribution to the theory of electrocapillarity. Philos Mag 1913;25:475–81.

Chia LS, Thompson JE, Moscarello MA. Disorder in human myelin induced by superoxide radical: an in vitro investigation. Biochem Biophys Res Commun 1983;117(1):141–6.

Chiu SY, Ritchie JM, Rogart RB, Stagg D. A quantitative description of membrane current in rabbit myelinated nerve. J Physiol 1979;292:149–66.

Chouard CH, Pialoux P. Biocompatibility of cochlear implants. Bull Acad Natl Med 1995;179(3):549–55.

Dautremont-Smith WC. Transition metal oxide electrochromic materials and displays: a review. Part 2. Oxides with anodic coloration. Displays 1982;3(3):67–80.

Delahay P. Double layer and electrode kinetics. New York: Interscience; 1965 [Chapters 2 and 7].

Donaldson PEK. The stability of tantalum-pentoxide films in vivo. Med Biol Eng 1974;12:131–5.

Donaldson NDN, Donaldson PEK. When are actively balanced biphasic (Lilly) stimulating pulses necessary in a neural prosthesis? I. Historical background, Pt resting potential, d*Q* studies. Med Biol Eng Comput 1986a;24:41–9.

Donaldson NDN, Donaldson PEK. When are actively balanced biphasic (Lilly) stimulating pulses necessary in a neural prosthesis? II. pH changes, noxious products, electrode corrosion, discussion. Med Biol Eng Comput 1986b;24:50–6.

Durand D. Bronzino JD, editor. Biomedical engineering handbook. Boca Raton: CRC Press; 1995 [Chapter 17].

Dymond AM, Kaechele LE, Jurist JM, Crandall PH. Brain tissue reaction to some chronically implanted metals. J Neurosurg 1970;33:574–80.

Fang Z, Mortimer JT. Selective activation of small motor axons by quasitrapezoidal current pulses. IEEE Trans Biomed Eng 1991a;38(2):168–74.

Fang Z, Mortimer JT. A method to effect physiological recruitment order in electrically activated muscle. IEEE Trans Biomed Eng 1991b;38(2):175–9.

Fisher G, Sayre GP, Bickford RC. Histological changes in the cat's brain after introduction of metallic and plastic-coated wire. In: Sheer DE, editor. Electrical stimulation of the brain. Austin: University of Texas Press; 1961. p. 55–9.

Frazer EJ, Woods R. The oxygen evolution reaction on cycled iridium electrodes. J Electroanal Chem 1979;102:127–30.

Furchgott RF. Studies on relaxation of rabbit aorta by sodium nitrite: the basis for the proposal that the acid-activatable inhibitory factor from retractor penis is inorganic nitrite and the endothelium-derived relaxing factor is nitric oxide, vasodilatation. In: Vascular smooth muscle, peptides, autonomic nerves and endothelium. New York: Raven Press; 1988 p. 401–14.

Ghai RS, Bikson M, Durand DM. Effects of applied electric fields on low-calcium epileptiform activity in the CA1 region of rat hippocampal slices. J Neurophysiol 2000;84(1):274–80.

Gileadi E, Kirowa-Eisner E, Penciner J. Interfacial electrochemistry: an experimental approach. Reading, MA: Addison-Wesley; 1975 [Section II].

Gluckman BJ, Neel EJ, Netoff TI, Ditto WL, Spano ML, Schiff SJ. Electric field suppression of epileptiform activity in hippocampal slices. J Neurophysiol 1996;76(6):4202–5.

Gorman PH, Mortimer JT. The effect of stimulus parameters on the recruitment characteristics of direct nerve stimulation. IEEE Trans Biomed Eng 1983;BME-30:407–14.

Gotman I. Characteristics of metals used in implants. J Endourol 1997;11(6):383–9.

Gottesfeld S. The anodic rhodium oxide film: a two-color electrochromic system. J Electrochem Soc 1980;127:272–7.

Grahame DC. The electrical double layer and the theory of electrocapillarity. Chem Rev 1947;41:441–501.

Greatbatch W, Chardack WM. Myocardial and endocardiac electrodes for chronic implantation. Ann N Y Acad Sci 1968;148:234–51.

Grill WM, Mortimer JT. Stimulus waveforms for selective neural stimulation. IEEE Eng Med Biol 1995;14:375–85.

Grill WM, Mortimer JT. Inversion of the current–distance relationship by transient depolarization. IEEE Trans Biomed Eng 1997;44(1):1–9.

Griot C, Vandevelde RA, Peterhans E, Stocker R. Selective degeneration of oligodendrocytes mediated by reactive oxygen species. Free Radic Res Commun 1990;11(4–5):181–93.

Guoy G. Constitution of the electric charge at the surface of an electrolyte. J Physique 1910;9:457–67.

Guyton DL, Hambrecht FT. Capacitor electrode stimulates nerve or muscle without oxidation–reduction reactions. Science 1973;181:74–6.

Guyton DL, Hambrecht FT. Theory and design of capacitor electrodes for chronic stimulation. Med Biol Eng 1974;7:613–20.

Halliwell B. Reactive oxygen species and the central nervous system. J Neurochem 1992;59(5):1609–23.

Hemnani T, Parihar MS. Reactive oxygen species and oxidative DNA damage. Indian J Physiol Pharmacol 1998;42(4):440–52.

Hille B. Ionic channels of excitable membranes. Sunderland, MA: Sinauer Associates; 1984.

Hodgkin AL, Huxley AF. Currents carried by sodium and potassium ions through the membrane of the giant axon of loligo. J Physiol 1952a;116:449–72.

Hodgkin AL, Huxley AF. The components of membrane conductance in the giant axon of logigo. J Physiol 1952b;116:473–96.

Hodgkin AL, Huxley AF. The dual effect of membrane potential on sodium conductance in the giant axon of logigo. J Physiol 1952c;116:497–506.

Hodgkin AL, Huxley AF. A quantitative description of the membrane current and its application to conduction and excitation in nerve. J Physiol 1952d;117:500–44.

Hoogerwerf AC, Wise KD. A three-dimensional microelectrode array for chronic neural recording. IEEE Trans Biomed Eng 1994;41:1136–46.

Ignarro LJ, Byrns RE, Wood KS. Biochemical and pharmacological properties of endothelium-derived relaxing factor and its similarity to nitric oxide radical. In: Vascular smooth muscle, peptides, autonomic nerves and endothelium. New York: Raven Press; 1988 p. 427–36.

Imlay JA. Pathways of oxidative damage. Annu Rev Microbiol 2003;57:395–418.

Ives DJG, Janz GJ. Reference electrodes: theory and practice. New York: Academic Press; 1961.

Johnson PF, Bernstein JJ, Hunter G, Dawson WW, Hench LL. An in vitro and in vivo analysis of anodized tantalum capacitive electrodes: corrosion response, physiology and histology. J Biomed Mater Res 1977;11:637–56.

Johnson PF, Hench LL. An in vitro analysis of metal electrodes for use in the neural environment. Brain Behav Evol 1977;14:23–45.

Jones KE, Campbell PK, Normann RA. A glass/silicon composite intracortical electrode array. Ann Biomed Eng 1992;20(4):423–37.

Kandel ER, Schwartz JH, Jessell TM. Principles of neural science. 4th ed. New York: McGraw-Hill; 2000.

Kelliher EM, Rose TL. Evaluation of charge injection properties of thin film redox materials for use as neural stimulation electrodes. Mater Res Soc Symp Proc 1989;110:23–7.

Kennedy PR. The cone electrode: a long-term electrode that records from neurites grown onto its recording surface. J Neurosci Methods 1989;29(3):181–93.

Kennedy PR, Bakay RA. Restoration of neural output from a paralyzed patient by a direct brain connection. Neuroreport 1998;9(8):1707–11.

Kennedy PR, Bakay RA, Moore M, Adams K, Montgomery G. Neural activity during acquisition of cursor control in a locked-in patient. Soc Neurosci Abstr 1999;25(1):894.

Klein JD, Clauson SL, Cogan SF. Morphology and charge capacity of sputtered iridium oxide films. J Vac Sci Technol A 1989;7:3043–7.

Konat G, Wiggins RC. Effect of reactive oxygen species on myelin membrane proteins. J Neurochem 1985;45:1113–8.

Kristensen BW, Noraberg J, Thiebaud P, Koudelka-Hep M, Zimmer J. Biocompatibility of silicon-based arrays of electrodes coupled to organotypic hippocampal brain slice cultures. Brain Res 2001;896:1–17.

Lagow CH, Sladek KJ, Richardson PC. Anodic insulated tantalum oxide electrocardiograph electrodes. IEEE Trans Biomed Eng 1971;18:162–4.

Lapicque L. Recherches quantitatives sur l'excitation electrique des nerfs traites comme une polarization. J Physiol (Paris) 1907;9:622–35.

Lilly JC, Austin GM, Chambers WW. Threshold movements produced by excitation of cerebral cortex and efferent fibers with some parametric regions of rectangular current pulses (cats and monkeys). J Neurophysiol 1952;15:319–41.

Lilly JC, Hughes JR, Alvord EC, Garkin TW. Brief noninjurious electric waveforms for stimulation of the brain. Science 1955;121:468–9.

Liu X, McCreery DB, Carter RR, Bullara LA, Yuen TGH, Agnew WF. Stability of the interface between neural tissue and chronically implanted intracortical microelectrodes. IEEE Trans Rehabil Eng 1999;7(3):315–26.

Loeb GE, Walker AE, Vematsu S, Konigsmark BW. Histological reaction to various conductive and dielectric films chronically implanted in the subdural space. J Biomed Mater Res 1977;11(2):195–210.

Loeb GE, Peck RA, Martyniuk J. Toward the ultimate metal microelectrode. J Neurosci Methods 1995;63:175–83.

Loucks RB, Weinberg H, Smith M. The erosion of electrodes by small currents. Electroencephalogr Clin Neurophysiol 1959;11:823–6.

Macquet JP, Theophanides T. DNA–platinum interactions. Characterization of solid DNA–$K_2[PtCl_4]$ complexes. Inorg Chim Acta 1976;18:189–94.

Majji AB, Humayun MS, Weiland JD, Suzuki S, D'Anna SA, deJuan Jr E. Long-term histological and electrophysiological results of an inactive epiretinal electrode array implantation in dogs. Invest Opthalmol Vis Sci 1999;40(9):2073–81.

McCreery DB, Bullara LA, Agnew WF. Neuronal activity evoked by chronically implanted intracortical microelectrodes. Exp Neurol 1986;92:147–61.

McCreery DB, Agnew WF, Yuen TGH, Bullara LA. Comparison of neural damage induced by electrical stimulation with Faradaic and capacitor electrodes. Ann Biomed Eng 1988;16:463–81.

McCreery DB, Agnew WF, Yuen TGH, Bullara LA. Charge density and charge per phase as cofactors in neural injury induced by electrical stimulation. IEEE Trans Biomed Eng 1990;37(10):996–1001.

McCreery DB, Agnew WF, Yuen TGH, Bullara LA. Damage in peripheral nerve from continuous electrical stimulation: comparison of two stimulus waveforms. Med Biol Eng Comput 1992a;30(1):109–14.

McCreery DB, Yuen TGH, Agnew WF, Bullara LA. Stimulation with chronically implanted microelectrodes in the cochlear nucleus of the cat: histologic and physiologic effects. Hear Res 1992b;62:42–56.

McHardy J, Geller D, Brummer SB. An approach to corrosion control during electrical stimulation. Ann Biomed Eng 1977;5:144–9.

McHardy J, Robblee RS, Marsten M, Brummer SB. Electrical stimulation with platinum electrodes. IV. Factors influencing platinum dissolution in inorganic saline. Biomaterials 1980;B1:129–34.

McIntyre CC, Grill WM. Extracellular stimulation of central neurons: influence of stimulus waveform and frequency on neuronal output. J Neurophysiol 2002;88(4):1592–604.

McIntyre CC, Thakor NV. Uncovering the mechanisms of deep brain stimulation for Parkinson's disease though functional imaging, neural recording, and neural modeling. Crit Rev Biomed Eng 2002;30(4–6):249–81.

McNeal DR. Analysis of a model for excitation of myelinated nerve. IEEE Trans Biomed Eng 1976;23(4):329–37.

Meyer RD, Cogan SF. Electrodeposited iridium oxide for neural stimulation and recording electrodes. IEEE Trans Neural Syst Rehabil Eng 2001;9(1):2–10.

Michael DJ, Wightman RM. Electrochemical monitoring of biogenic amine neurotransmission in real time. J Pharm Biomed Anal 1999;19:33–46.

Moncada S, Palmer RMJ, Higgs EA. Nitric oxide: physiology, pathology and pharmacology. Pharmacol Rev 1991;43(2):109–42.

Mortimer JT, Shealy CN, Wheeler C. Experimental nondestructive electrical stimulation of the brain and spinal cord. J Neurosurg 1970;32(5):553–9.

Mortimer JT, Kaufman D, Roessmann U. Intramuscular electrical stimulation: tissue damage. Ann Biomed Eng 1980;8:235–44.

Mortimer JT. Agnew WF, McCreery DB, editors. Neural prostheses: fundamental studies. Prentice-Hall: Englewood Cliffs; 1990 [Chapter 3].

Morton SL, Daroux ML, Mortimer JT. The role of oxygen reduction in electrical stimulation of neural tissue. J Electrochem Soc 1994;141:122–30.

Mozota J, Conway BE. Surface and bulk processes at oxidized iridium electrodes. I. Monolayer stage and transition to reversible multilayer oxide film behavior. Electrochim Acta 1983;28:1–8.

Niparko JK, Altschuler RA, Xue XL, Wiler JA, Anderson DJ. Surgical implantation and biocompatibility of central nervous system auditory prostheses. Ann Otol Rhinolaryngol 1989;98(12 Part 1):965–70.

O'Suilleabhain PE, Frawley W, Giller C, Dewey RB. Tremor response to polarity, voltage, pulsewidth and frequency of thalamic stimulation. Neurology 2003;60(5):786–90.

Pletcher D, Walsh FC. Industrial electrochemistry. 2nd edition. London: Chapman & Hall; 1990 [Section 1.3].

Plonsey R, Barr RC. Bioelectricity: a quantitative approach. New York: Plenum Press; 1988. p. 144.

Pudenz RH, Bullara LA, Dru D, Talalla A. Electrical stimulation of the brain. II. Effects on the blood–brain barrier. Surg Neurol 1975a;4:265–70.

Pudenz RH, Bullara LA, Jacques P, Hambrecht FT. Electrical stimulation of the brain. III. The neural damage model. Surg Neurol 1975b;4:389–400.

Radomski MW, Palmer RMJ, Moncada S. Endogenous nitric oxide inhibits human platelet adhesion to vascular endothelium. Lancet 1987;2:1057–8.

Rall W. Handbook of physiology—the nervous system I, vol.1/part 1. American Physiological Society; 1977 [Chapter 3].

Ranck JB, Patterson MM, Kesner RP, editors. Electrical stimulation research techniques. New York: Academic Press; 1981 [Chapter 1].

Rand DAJ, Woods R. The nature of adsorbed oxygen on rhodium, palladium, and gold electrodes. J Electroanal Chem Interfacial Electrochem 1971;31:29–38.

Rand DAJ, Woods R. Cyclic voltammetric studies on iridium electrodes in sulfuric acid solutions. Nature of oxygen layer and metal dissolution. J Electroanal Chem Interfacial Electrochem 1974;55:375–81.

Randles JEB. Rapid electrode reactions. Discuss Faraday Soc 1947;1:11–9.

Rattay F. Analysis of models for extracellular fiber stimulation. IEEE Trans Biomed Eng 1989;36:676–82.

Robblee RS, McHardy J, Marsten M, Brummer SB. Electrical stimulation with platinum electrodes. V. The effects of protein on platinum dissolution. Biomaterials 1980;B1:135–9.

Robblee RS, Lefko JL, Brummer SB. Activated iridium: an electrode suitable for reversible charge injection in saline solution. J Electrochem Soc 1983a;130:731–3.

Robblee RS, McHardy J, Agnew WF, Bullara LA. Electrical stimulation with Pt electrodes. VII. Dissolution of Pt electrodes during electrical stimulation of the cat cerebral cortex. J Neurosci Methods 1983b;9:301–18.

Robblee LS, Mangaudis MM, Lasinsky ED, Kimball AG, Brummer SB. Charge injection properties of thermally-prepared iridium oxide films. Mater Res Soc Symp Proc 1986;55:303–10.

Robblee LS, Rose TL. Electrochemical guidelines for selection of protocols and electrode materials for neural stimulation. In: Agnew

WF, McCreery DB, editors. Neural prostheses: fundamental studies. Prentice-Hall: Englewood Cliffs; 1990. p. 25–66.

Rose TL, Kelliher EM, Robblee LS. Assessment of capacitor electrodes for intracortical neural stimulation. J Neurosci Methods 1985;12(3):181–93.

Rose TL, Robblee LS. Electrical stimulation with Pt electrodes. VIII. Electrochemically safe charge injection limits with 0.2 ms pulses. IEEE Trans Biomed Eng 1990;37(11):1118–20.

Rosenberg B, VanCamp L, Krigas T. Inhibition of cell division in *Escherichia coli* by electrolysis products from a platinum electrode. Nature 1965;205:698–9.

Rosenberg B. Some biological effects of platinum compounds: new agents for the control of tumours. Platinum Met Rev 1971;15:42–51.

Rousche PJ, Pellinen DS, Pivin DP, Williams JC, Vetter RJ, Kipke DR. Flexible polyimide-based intracortical electrode arrays with bioactive capability. IEEE Trans Biomed Eng 2001;48(1):361–70.

Rubanyi GM. Vascular effects of oxygen derived free radicals. Free Radic Biol Med 1988;4:107–20.

Rudge JS, Smith GM, Silver J. An in vitro model of wound healing in the central nervous system: analysis of cell reaction and interaction at different times. Exp Neurol 1989;103:1–16.

Ryhanen J, Kallioinen M, Tuukkanen J, Junila J, Niemela E, Sandvik P, et al. In vivo biocompatibility evaluation of nickel–titanium shape memory alloy: muscle and perineural tissue responses and encapsule membrane thickness. J Biomed Mater Res 1998;41(3):481–8.

Sawyer PN, Srinivasan S. In: Ray CD, editor. Medical engineering. Chicago: Year Book Medical Publishers; 1974. p. 1099–110.

Scheiner A, Mortimer JT. Imbalanced biphasic electrical stimulation: muscle tissue damage. Ann Biomed Eng 1990;18:407–25.

Schmidt S, Horch K, Normann R. Biocompatibility of silicon-based electrode arrays implanted into feline cortical tissue. J Biomed Mater Res 1993;27(11):1393–9.

Sevanian A. Lipid peroxidation, membrane damage, and phospholipase A2 action: cellular antioxidant defense mechanisms. CRC Rev 1988;II:77–95.

Shannon RV. A model of safe levels for electrical stimulation. IEEE Trans Biomed Eng 1992;39(4):424–6.

Shepherd RK, Murray MT, Houghton ME, Clark GM. Scanning electron microscopy of chronically stimulated platinum intracochlear electrodes. Biomaterials 1985;6:237–42.

Silbey RJ, Alberty RA. Physical chemistry. 3rd ed. New York: Wiley; 2001.

Stieglitz T, Meyer JU. Implantable Microsystems. Polyimide-based neuroprostheses for interfacing nerves. Med Dev Technol 1999;10(6):28–30.

Stensaas SS, Stensaas LJ. Histopathological evaluation of materials implanted in the cerebral cortex. Acta Neuropathol (Berl) 1978;41:145–55.

Stern O. Zur theorie der elektrolytischen doppelschicht. Z Elektrochem 1924;30:508–16.

Stohs SJ. The role of free radicals in toxicity and disease. J Basic Clin Physiol Pharmacol 1995;6(3–4):205–28.

Sweeney JD, Durand D, Mortimer JT. Modeling of mammalian myelinated nerve for functional neuromuscular stimulation. In: Proceedings of the Ninth International Conference of IEEE-EMBS; 1987. p. 1577–8.

Tivol WF, Agnew WF, Alvarez RB, Yuen TGH. Characterization of electrode dissolution products on the high voltage electrode microscope. J Neurosci Methods 1987;19:323–37.

Turner JN, Shain W, Szarowski DH, Andersen M, Martins S, Isaacson M, et al. Cerebral astrocyte response to micromachined silicon implants. Exp Neurol 1999;156:33–49.

Umans J, Levi R. Nitric oxide in the regulation of blood flow and arterial pressure. Annu Rev Physiol 1995;57:771–90.

van den Honert C, Mortimer JT. Generation of unidirectionally propagated action potentials in a peripheral nerve by brief stimuli. Science 1979;206(4424):1311–2.

van den Honert C, Mortimer JT. A technique for collision block of peripheral nerve: single stimulus analysis. IEEE Trans BME 1981a;28:373–8.

van den Honert C, Mortimer JT. A technique for collision block of peripheral nerve: frequency dependence. IEEE Trans BME 1981b;28:379–82.

von Helmholtz HLF. Ueber einige gesetze der vertheilung elektrischer strome in korperlichen leitern mit anwendung auf die thierisch-elektrischen versuche. Ann Phys 1853;89:211–33.

Warman EN, Grill WM, Durand D. Modeling the effects of electric fields on nerve fibers: determination of excitation thresholds. IEEE Trans Biomed Eng 1992;39(12):1244–54.

Weiland JD, Anderson DJ. Chronic neural stimulation with thin-film, iridium oxide electrodes. IEEE Trans Biomed Eng 2000;47(7):911–8.

Weinman J, Mahler J. An analysis of electrical properties of metal electrodes. Med Electron Biol Eng 1964;2:229–310.

White RL, Gross TJ. An evaluation of the resistance to electrolysis of metals for use in biostimulation probes. IEEE Trans Biomed Eng 1974;BME-21:487–90.

Wiley JD, Webster JJ. Analysis and control of the current distribution under circular dispersive electrodes. IEEE Trans Biomed Eng 1982;BME-29:381–5.

Yuen TGH, Agnew WF, Bullara LA, Jacques S, McCreery DB. Histological evaluation of neural damage from electrical stimulation: considerations for the selection of parameters for clinical application. Neurosurgery 1981;9(3):292–9.

Zerbino JO, Tacconi NR, Arvia AJ. The activation and deactivation of iridium in acid electrolytes. J Electrochem Soc 1978;125:1266–76.